

## REVIEW OPEN ACCESS

# Smart Flexible Tactile Sensors: Recent Progress in Device Designs, Intelligent Algorithms, and Multidisciplinary Applications

Siyuan Wang<sup>1,2,3</sup> | Ming Dong<sup>4,5</sup> | Rongrong Bao<sup>1,2</sup> | Caofeng Pan<sup>1,2</sup> 

<sup>1</sup>Institute of Atomic Manufacturing, Beihang University, Beijing, China | <sup>2</sup>International Research Institute for Multidisciplinary Science, Beihang University, Beijing, China | <sup>3</sup>School of Physics, Beihang University, Beijing, China | <sup>4</sup>Beijing Institute of Tracking and Telecommunications Technology, Beijing, China | <sup>5</sup>Key Laboratory of Smart Earth, Beijing, China

**Correspondence:** Rongrong Bao ([baorongrong@buaa.edu.cn](mailto:baorongrong@buaa.edu.cn)) | Caofeng Pan ([pancaofeng@buaa.edu.cn](mailto:pancaofeng@buaa.edu.cn))

**Received:** 9 July 2025 | **Revised:** 30 September 2025 | **Accepted:** 1 October 2025

**Funding:** National Natural Science Foundation of China, Grant/Award Numbers: 62422120 52371202 52192610 52125205 52250398 52203307; Natural Science Foundation of Beijing, Grant/Award Number: L223006; Shenzhen Science and Technology Program, Grant/Award Number: KQTD20170810105439418; Fundamental Research Funds for the Central Universities

**Keywords:** flexible tactile sensors | intelligent algorithms | intelligent tactile systems | smart sensors

## ABSTRACT

Flexible tactile sensors, leveraging their deformability, low elastic modulus, and high sensitivity, have emerged as pivotal technologies in healthcare monitoring, human-machine interfaces, and bioinspired robotics. This review systematically examines advancements in wearable flexible pressure sensors, focusing on device designs, performance optimization strategies, and intelligent application paradigms. A critical focus of our analysis is on how artificial-intelligence-driven algorithms assist sensors in overcoming key challenges such as noise suppression, feature extraction, and environmental adaptability, leading to significantly enhanced perception accuracy and decision-making autonomy in dynamic scenarios. The synergistic integration of sensing and computation is highlighted as a transformative approach for emerging applications like embodied intelligent navigation and adaptive motion control. Furthermore, existing technical barriers are identified, including challenges in device integration and computing latency, offering a roadmap for interdisciplinary innovation and industrial translation of next-generation intelligent tactile systems.

## 1 | Introduction

Flexible tactile sensors, as emerging electronic devices fabricated from compliant materials, enable pressure-to-electrical signal transduction, thereby achieving biomimetic tactile sensing functionalities [1, 2]. Compared to conventional rigid pressure sensors based on metals, piezoelectric crystals, or semiconductors, flexible counterparts exhibit distinct advantages including mechanical deformability, superior conformability to irregular surfaces [3, 4], rapid response kinetics, high sensitivity, and enhanced spatial resolution [5]. Notably, certain stretchable flexible sensors also exhibit low elastic modulus and high stretchability. They can retain

accurate pressure sensing capabilities while being stretched, granting them superior adaptability to various environments. These attributes have established their pivotal role in tactile perception [6], healthcare monitoring [7, 8], human-machine interfaces [9, 10], internet of things [11], sports analytics [12], electronic skin [13], and biorobotics [14], positioning them as a cornerstone technology for wearable and humanoid sensing applications. As these sensing technologies approach maturity, they function like sensory organs that generate vast data but lack the ‘brain’ to interpret it effectively. The introduction of AI algorithms acts as this cognitive layer, providing essential functions like pattern recognition, environmental adaptation, and autonomous learning, which are

Siyuan Wang and Ming Dong contributed equally to this study.

This is an open access article under the terms of the [Creative Commons Attribution](https://creativecommons.org/licenses/by/4.0/) License, which permits use, distribution and reproduction in any medium, provided the original work is properly cited.

© 2025 The Author(s). *Advanced Intelligent Discovery* published by Wiley-VCH GmbH.

critical for advancing intelligent data processing, multidimensional analysis, and application diversification. The integration of intelligent algorithms has endowed flexible pressure sensors with adaptive cognition capabilities, driving their evolution into a prominent research frontier for next-generation wearable systems [15, 16].

The advancement of intelligent processing relies on artificial intelligence (AI) methodologies, particularly machine learning (ML) and deep learning (DL) paradigms encompassing supervised, unsupervised, and reinforcement learning. These approaches have demonstrated transformative success in medical imaging diagnostics, autonomous systems, quantitative finance, intelligent logistics, large language models, and biometric recognition [17–19]. For wearable pressure sensing, intelligent algorithms iteratively extract decision-making rules from sensor data, emulating human-like environmental adaptation to enhance both sensing accuracy and application efficacy [20, 21]. Specifically, they address critical challenges such as data redundancy, noise interference, environmental variability, and feature ambiguity, thereby improving signal-to-noise ratios (SNRs) and enabling robust interference isolation [22–24]. Moreover, given the dynamic and interactive nature of tactile sensing environments, intelligent algorithms transcend passive data analysis to facilitate active sensor-environment interactions [25]. This paradigm bridges flexible sensing with embodied intelligence systems, fostering innovations in motion pattern recognition, real-time haptic feedback control, and context-aware navigation through predictive analytics [15, 16, 26–28].

This review comprehensively examines recent advancements in flexible tactile sensors and intelligent algorithms for pressure sensing applications. As depicted in Figure 1, intelligent flexible tactile sensors typically employ resistive [29], capacitive [33], piezoelectric [34], or triboelectric [35] transduction mechanisms, coupled with signal conditioning circuits and ML-driven data processing pipelines [30], to enable applications in health monitoring [31], human-machine interface [32], and intelligent robotics [27]. We first systematically analyze the device architectures, operational principles, and classification frameworks of flexible tactile sensors, followed by proposing standardized performance metrics and summarizing cutting-edge innovations. Subsequently, we critically evaluate the implementation strategies and current progress of intelligent algorithms in addressing sensor-specific limitations. Detailed case studies highlight application breakthroughs across representative scenarios. Finally, we delineate persistent technical challenges and propose multidisciplinary research directions to guide the development of intelligent tactile sensing systems.

## 2 | Flexible Tactile Sensing Technologies

This chapter reviews recent advancements in flexible tactile sensors from a device-oriented perspective. Beginning with a systematic analysis of fundamental architectures and common material systems employed in sensor design, we subsequently elucidate

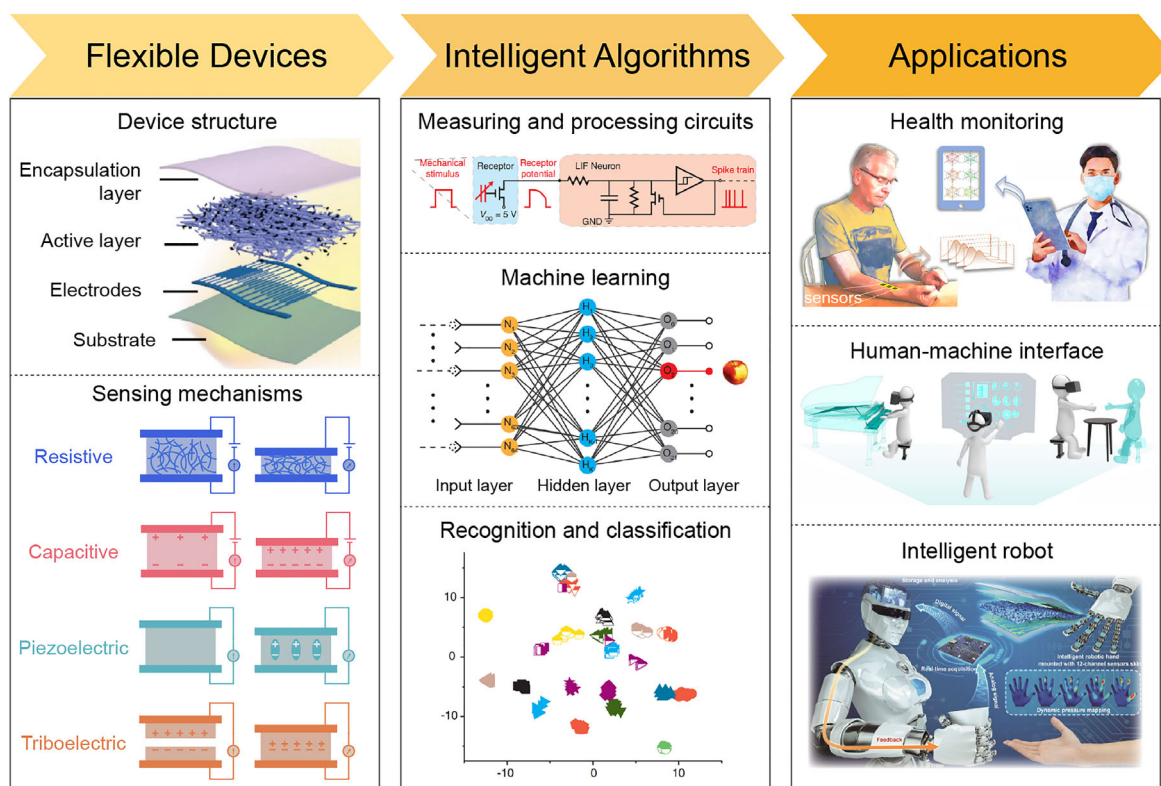


**FIGURE 1** | Schematic overview of the flexible tactile sensing system: from devices to intelligent algorithms to applications. Top left. Reproduced with permission [29]. Copyright 2022, John Wiley and Sons. Middle. Reproduced with permission [30]. Copyright 2024, The American Association for the Advancement of Science. Top right. Reproduced under terms of the CC-BY license [31]. Copyright 2023, American Chemical Society. Middle right. Reproduced under terms of the CC-BY license [32]. Copyright 2022, Springer Nature. Bottom right. Reproduced with permission [27]. Copyright 2023, Elsevier.

prevalent tactile sensing mechanisms, including their operational principles and implementation strategies. Concluding with a critical evaluation, we establish a comprehensive framework of standardized performance metrics to guide the characterization and optimization of next-generation tactile sensing technologies.

## 2.1 | The Basic Composition of a Sensor

Flexible pressure sensors are primarily composed of a flexible substrate, active layer, conductive electrode, and encapsulation layer [36, 37]. The flexible substrate provides essential support and a conformal contact interface, requiring elasticity, tensile strength, and adhesion. Materials must offer key properties: conformal deformation capability, long-term durability, robust environmental resistance, and seamless compatibility with integrated sensors [38]. The active layer transforms mechanical deformation into electrical signals through structural changes. For example, pressure changes capacitance in the dielectric layer of capacitive sensors, while it forms conductive paths to lower resistivity in the conductive elastomer of piezoresistive sensors.

The electrode must maintain electrical stability under mechanical stress, necessitating specialized material/structural designs compared to rigid sensors. The encapsulation layer enhances operational robustness and may introduce secondary functionalities like self-healing. This section reviews recent advancements in these four components.

### 2.1.1 | Flexible Substrate

The flexible substrate constitutes the fundamental architecture of flexible pressure sensors, enabling the integration of electrodes and sensing layers to achieve mechanical compliance and stretchability, while ensuring conformal contact with irregular surfaces in complex environments [38–40]. Common materials for flexible tactile sensors include polydimethylsiloxane (PDMS) [41, 42], polyimide (PI) [43, 44], polyethylene terephthalate (PET) [45], hydrogels [46], and nanofiber materials [47] as flexible substrates. Among these, nanofiber films have garnered significant attention as a promising substrate for wearable devices due to their exceptional flexibility, mechanical strength, and breathability. For instance, Pan's group reported a gas-spinning

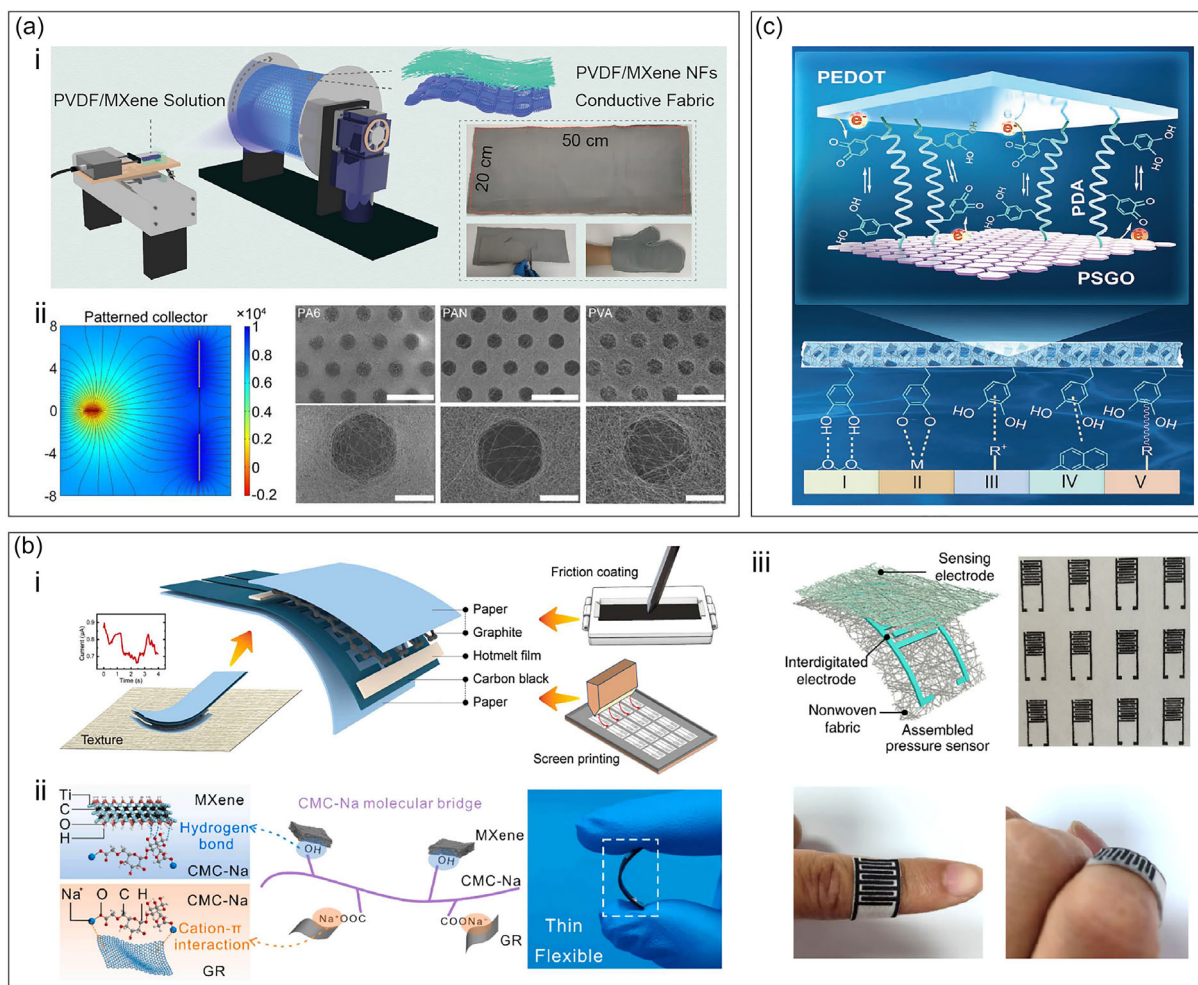


**FIGURE 2** | Substrate for flexible tactile sensors. (a) Nanofiber substrates. i) Large-area electrospun film. Reproduced with permission [48]. Copyright 2022, John Wiley and Sons. ii) Nanofiber substrates with controllable modulus. Reproduced with permission [49]. Copyright 2023, Elsevier. (b) Biocompatible substrates. i) Paper-based substrate. Reproduced with permission [50]. Copyright 2024, Elsevier. ii) Cellulose paper substrate. Reproduced with permission [51]. Copyright 2024, Elsevier. iii) Nonwoven fabric substrate. Reproduced under terms of the CC-BY license [52]. Copyright 2024, John Wiley and Sons. (c) Hydrogel-based substrate. Reproduced with permission [53]. Copyright 2019, John Wiley and Sons.



technique to fabricate large-area ( $20 \times 50 \text{ cm}^2$ ) polyvinylidene difluoride (PVDF)/MXene composite nanofiber films [48], as illustrated in Figure 2a-i. This solvent-gas spinning method enables scalable roll-to-roll manufacturing, eliminates high-voltage requirements, and allows versatile substrate selection. The resulting breathable films can be tailored into wearable devices (e.g., gloves) via cutting and stitching. In 2023, their group advanced this technology by introducing patterned electrospinning to spatially control the Young's modulus of nanofiber substrates (Figure 2a-ii) [49]. By designing collectors with varied pore sizes to modulate electric field distributions, they achieved controlled fiber deposition and micron-scale pore formation, thereby tailoring mechanical properties for specific applications. The patterned nanofiber composite network exhibits ultrathin and stretchable characteristics, ensuring reliable skin contact during mechanical deformation to prevent signal distortion. This method has been successfully extended to various nanofibers.

The demand for biocompatible substrates has surged with the rapid development of wearable technologies. Traditional materials like paper and nonwoven fabrics offer proven safety for long-term wear. Chen et al. [50] developed an ultralight (6 mg), low-cost paper-based pressure sensor using water-soluble graphite ink (Figure 2b-i). The sensor, featuring a graphite functional layer and carbon interdigitated electrodes, demonstrated high sensitivity and achieved high accuracy in surface texture recognition. Similarly, Zhang et al. [51] fabricated a dual-mode temperature/pressure sensor by impregnating cellulose paper with sodium carboxymethyl cellulose-stabilized conductive fillers (Figure 2b-ii). The device exhibited rapid response/recovery times (37.5 ms), showing potential for gesture tracking and sleep monitoring. Li et al. [52] employed screen printing to deposit MXene/PEDOT:PSS (Poly (3,4-ethylenedioxythiophene)-poly (styrenesulfonate)) composite ink on nonwoven fabric (Figure 2b-iii), where PEDOT:PSS effectively prevented MXene oxidation, enhancing sensitivity ( $754.5 \text{ kPa}^{-1}$ ) and cyclic stability ( $>1000$  cycles).

Hydrogels have emerged as a research frontier in flexible sensing owing to their intrinsic flexibility, conductivity, self-healing, biocompatibility, and adhesion properties [46, 53]. As shown in Figure 2c, Lu's team designed a hydrogel with redox-active catechol/quinone bonds derived from dopamine, enabling durable adhesion to ceramics, metals, and biological tissues for stable in vivo electrophysiological signal acquisition [53].

### 2.1.2 | Active Layer

The active layer constitutes the core component of pressure sensing systems, responsible for converting external mechanical stimuli into electrical signals. Depending on the transduction mechanism, this layer is typically composed of elastic materials or structures with dielectric, conductive, or piezoelectric/triboelectric properties [54–58]. For instance, piezoresistive layers are often fabricated by embedding conductive fillers such as graphene, carbon nanotubes (CNTs), MXene, or conductive polymers (e.g., PEDOT:PSS) into elastomeric matrices or nanofiber networks. Current research priorities focus on enhancing conductivity, sensitivity, and mechanical stability. A notable example is the work by Xu et al. [59], who designed an ultralight

MXene-based aerogel using nanocellulose and bioinspired textures, achieving a linear sensitivity of  $817.3 \text{ kPa}^{-1}$ . This material simultaneously served as a compressible supercapacitor electrode, suitable for epidermal monitoring and motion detection. In another advancement, Yasuda et al. [60] synthesized functional polymer nanoparticles to develop an electret-based flexible pressure sensor with an ultrafast response time of 4 ms and a high sensitivity. Yang et al. [61] leveraged naturally formed ultrathin alumina ( $\text{Al}_2\text{O}_3$ ) as a dielectric layer, suppressing electron tunneling via the Schottky effect to achieve a high unit-area capacitance of  $50 \text{ nF cm}^{-2}$ . By integrating hollow hemispherical microstructures, their sensor exhibited a sensitivity of  $8.6 \text{ kPa}^{-1}$  and a broad linear range of 50 kPa, showing promise for wearable and robotic applications. Chen et al. [62] proposed a polyamide-imide (PAI)/polyaniline (PANI) composite piezoresistive sensor, where the in situ polymerized PANI semiconductor layer on PAI fibers provided high anticreep stability. The sensor achieved a linear sensitivity of  $35.3 \text{ kPa}^{-1}$  within 0.2–20 kPa, with minimal signal drift (3.8% after 10 000 cycles), enabling real-time pressure mapping for smart gesture recognition and posture monitoring. Further innovations include He et al. [63], who developed a nanostructured ionogel via photopolymerization-induced microphase separation. This material exhibited exceptional ionic conductivity ( $>3 \text{ S m}^{-1}$ ), extreme stretchability ( $>1500\%$ ), and thermal stability (from  $-72$  to  $250^\circ\text{C}$ ), compatible with 3D-printed microstructures for capacitive sensing applications.

### 2.1.3 | Electrode

The conductive electrode is responsible for collecting and transmitting electrical signals generated by the active layer. Common electrode materials must exhibit high conductivity and stability [64], including metallic materials (e.g., metal nanoparticles, nanowires, inks) [65–69], carbon-based materials (e.g., CNTs, graphene) [70], inorganic compound (e.g., MXene) [71], and organic conductors (e.g., PEDOT:PSS) [72, 73]. Among these, metallic materials remain the most extensively studied due to their superior conductivity, ductility, and accessibility. Recent research has focused on enhancing the electrical and mechanical stability of electrodes under strain. For example, Cao et al. [66] reported an interfacial diffusion-induced cohesion strategy, where hydrophilic polyurethane was used to wet gold (Au) particles and encapsulate them via strong hydrogen bonding, achieving exceptional interfacial adhesion. By further constructing nanoscale rough structures with rigid polyurethane, the adhesion strength was enhanced to 100 times that of traditional PDMS-based devices and four times that of styrene-ethylene-butylene-styrene (SEBS)-based devices. The resulting electrode maintained stable conductivity and reliability even after 1,022 friction cycles under 130 kPa pressure, enabling pressure sensors with superior mechanical durability for high-load applications. Jiang et al. [67] developed a highly stretchable hybrid interface using interpenetrating metal-polymer nanostructures, which integrated soft, rigid, and encapsulated modules into continuous mechanical and electrical pathways via a plug-and-play design. This approach achieved soft interconnects with outstanding electrical ( $>180\%$ ) and mechanical ( $>600\%$ ) stretchability.

Liquid metals (LMs), recognized for their room-temperature conductivity and deformability, have emerged as a research

frontier. They serve as ideal electrode materials that maintain electrical stability under extreme mechanical deformation, enabling reliable signal transmission in dynamically bending interfaces [69]. Zheng et al. [74] proposed a method to fabricate LM-embedded fibrous films via a pressure-stamping technique. LM particles were semi-embedded into electrospun polymer fiber networks with diameter-matched configurations. Under pressure, the LM shells ruptured to fill fiber gaps, forming conductive networks. Internally anchored LM particles and surface-bonded LM-nanofiber interactions improved interfacial compatibility, yielding flexible electronics with high resolution (minimum linewidth: 100  $\mu\text{m}$ ) and cyclic stability (>30000 cycles). Chen et al. [75] designed a compressible and stretchable biphasic liquid–solid self-healing circuit by filling micropillar-embedded channels with GaInSn–BiInSn dual-phase metals. The underlying BiInSn solid alloy acted as a compression-resistant layer, while the upper GaInSn liquid metal autonomously filled cracks in the solid layer during large deformations, achieving self-healing conductivity under both tensile and compressive strains.

#### 2.1.4 | Encapsulation Layer

The encapsulation layer protects the sensor's internal structure and isolates external environmental interference. Traditional encapsulation materials, such as silicone rubbers and polyester films, are widely used to ensure operational robustness, reliability, and environmental adaptability of sensors [76–83]. For example, Yan et al. [84] developed a single-fiber piezoelectric sensor using SEBS as an elastic encapsulation layer, which converted mechanical vibrations into electrical signals for microphone applications. Hu et al. [85] reported a salt-resistant swelling hydrogel for encapsulating flexible devices to enhance their applicability in marine environments. The hydrogel's carboxyl and methoxy groups, combined with octopus-sucker-inspired surface microstructures, enabled robust adhesion to various materials. The synergistic interplay between hydrophobic and hydrophilic domains in its network structure further provided exceptional antistretching capability in saline conditions. Recent studies also reveal that encapsulation can confer novel functionalities beyond protection. Yu's team engineered a spatially heterogeneous wettability encapsulation layer to direct sweat drainage, maintaining stable and comfortable skin-device interfaces during perspiration, thereby enabling seamless, continuous, and thermally comfortable health monitoring [86].

Self-healing properties have emerged as another critical research direction, achievable through advanced encapsulation materials [87]. Cooper et al. [54] utilized two immiscible yet dynamically bonded polymers (polypropylene glycol hyperbranched polymer and polydimethylsiloxane hyperbranched polymer) to enable automatic realignment and repair of damaged multilayer flexible substrates. This approach offers technical solutions for pressure sensors, soft robotic magnetic assemblies, and underwater circuits in complex environments. Cheng et al. [88] constructed high-strength MXene sheets reinforced by hydrogen bonds between 1D aramid nanofibers, achieving a flexible pressure sensor with outstanding self-healing performance. The MXene sheets with 30% aramid nanofibers exhibited tensile strength and toughness 712% and 3347% higher than pure MXene, respectively.

## 2.2 | Sensing Mechanisms

Flexible pressure sensors can be categorized into four primary types based on their sensing mechanisms: resistive, capacitive, piezoelectric, and triboelectric. Among these, resistive and capacitive sensors dominate research efforts due to their structural simplicity, stable signal output, and straightforward signal acquisition circuit design [89]. In contrast, self-powered piezoelectric and triboelectric sensors have garnered increasing research attention in recent years owing to their low energy consumption and potential to address energy harvesting challenges in distributed sensing systems. This section systematically reviews the current advancements in these four sensing modalities.

### 2.2.1 | Resistive Sensors

Resistive pressure sensors operate through resistance changes in materials under external mechanical stress. When pressure is applied, the deformation of the sensing layer (typically composed of conductive fillers embedded in an elastic matrix) alters the internal conductive network. For instance, increased contact area or new conductive pathways between particles (e.g., CNTs, graphene, or metal nanoparticles) reduce overall resistance. Recent research focuses on enhancing sensitivity, response speed, and wearability through novel materials and microstructural designs.

Jiang et al. [90] developed a machine-knitted resistive sensor with a triaxial spacer fabric structure (Figure 3a-i), capable of detecting vertical pressure and horizontal strain while seamlessly integrating with textiles for human motion monitoring. Zheng et al. [94] created a fully paper-based resistive sensor using blade-coated porous composite electrodes and screen-printed copper electrodes, achieving high sensitivity ( $1014 \text{ kPa}^{-1}$ ) and a broad detection range (up to 300 kPa) for signals ranging from wrist pulses to forceful finger taps. Xiang et al. [70] designed a metal-free, biocompatible resistive sensor (Figure 3a-ii) featuring a dual-sided pyramidal carbon aerogel sensing layer and silicone frame. This device demonstrated high sensitivity ( $37.3 \text{ kPa}^{-1}$ ), wide linearity (0–1.4 MPa), and >30 000-cycle stability, showing versatile application potential.

### 2.2.2 | Capacitive Sensors

Capacitive sensors detect pressure-induced changes in capacitance via alterations in electrode spacing, overlap area, or dielectric constant. Their advantages include noncontact measurement, high resolution, temperature stability, and low power consumption. Recent advances leverage electric double layers at ion-conductor/electron-conductor interfaces for enhanced sensitivity.

Yuan et al. [95] synthesized a leakage-free polyelectrolyte elastomer with micropillar arrays as the dielectric layer, achieving a sensitivity of  $69.6 \text{ kPa}^{-1}$  and stability under static/dynamic loads up to 1 MPa. Sun et al. [96] designed a supercapacitive ionic sensor with thermoplastic polyurethane/MXene nanofiber electrodes sandwiching a porous polyurethane/ionic liquid sponge, yielding a sensitivity of  $105.77 \text{ kPa}^{-1}$ . Wu et al. [97] developed a stretchable all-nanofiber ionic sensor using liquid metal electrodes, achieving  $1.08 \text{ kPa}^{-1}$  sensitivity and rapid response/

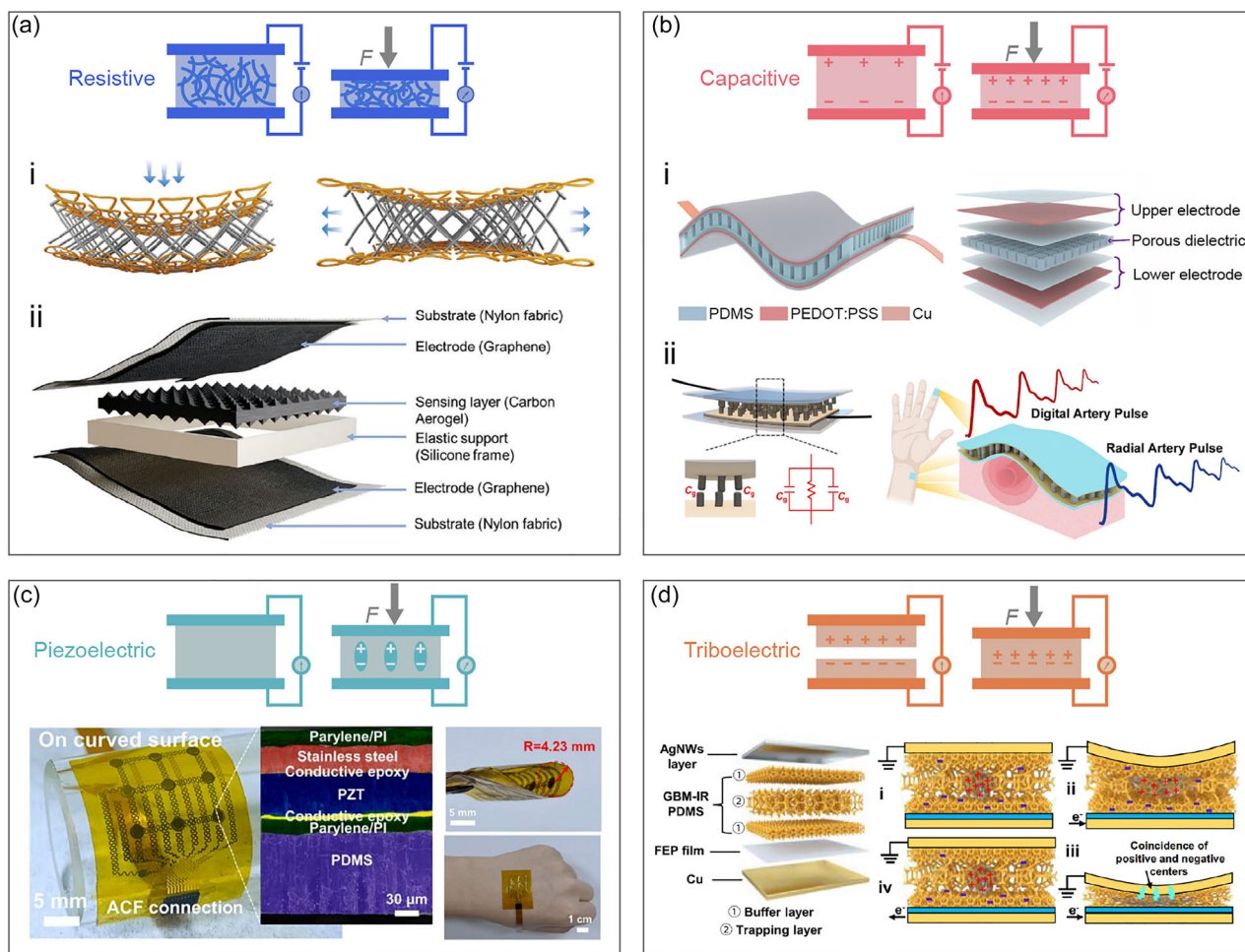


**FIGURE 3** | Sensing mechanisms. (a) Resistive sensors. i) Resistive sensor with a triaxial spacer fabric structure. Reproduced with permission [90]. Copyright 2023, American Chemical Society. ii) Paper-based resistive sensor. Reproduced with permission [70]. Copyright 2024, John Wiley and Sons. (b) Capacitive sensors. i) Capacitive sensor with 3D-printed porous dielectric microstructures. Reproduced with permission [91]. Copyright 2024, American Chemical Society. ii) Hybrid capacitive-resistive sensor with face-to-face conductive micropillar arrays. Reproduced with permission [89]. Copyright 2023, Royal Society of Chemistry. (c) Piezoelectric sensors. Reproduced with permission [92]. Copyright 2024, Elsevier. (d) Triboelectric sensors. Reproduced under terms of the CC-BY license [93]. Copyright 2024, Springer Nature.

relaxation (18/22 ms), validated in soft pneumatic gripper tests. Li et al. [91] engineered a high-performance capacitive sensor (Figure 3b-i) via 3D-printed porous dielectric microstructures, demonstrating  $0.21 \text{ kPa}^{-1}$  sensitivity and  $>455.2 \text{ kPa}$  interfacial strength with minimal performance variation across arrays. Shen et al. [89] reported a hybrid capacitive-resistive sensor (Figure 3b-ii) with face-to-face conductive micropillar arrays, enabling high sensitivity across five orders of magnitude for acoustic pressure, arterial pulses, and joint motion detection.

### 2.2.3 | Piezoelectric/Triboelectric Sensors

Self-powered piezoelectric/triboelectric sensors are gaining traction for distributed sensing due to their low energy consumption and dynamic force detection capabilities. Wang et al. [98] synthesized a piezoelectric hydrogel via acrylamide-acrylonitrile copolymerization, achieving  $0.51 \text{ MPa}$  tensile strength and  $0.2 \text{ V kPa}^{-1}$  sensitivity for mechanoelectrical conversion. Zhang et al. [99] fabricated hollow PVDF nanofibers via coaxial electrospinning, producing a sensor with 56.9% strain tolerance

and  $2.7 \text{ V/N}$  sensitivity. Zhen et al. [92] designed a flexible piezoelectric array (Figure 3c) combining ceramic powders and polymer films, achieving  $6 \text{ mm}$  spatial resolution,  $4.23 \text{ mm}$  bending radius, and  $15.08 \text{ mV/kPa}$  sensitivity for motion tracking and voice recognition. Qin et al. [93] developed a triboelectric sensor (Figure 3d) with water-rich elastomers and gradient microchannels, resolving the sensitivity-linearity trade-off to achieve a record-wide linear range ( $5\text{--}1240 \text{ kPa}$ ) and  $0.023 \text{ V kPa}^{-1}$  sensitivity, advancing practical applications.

## 2.3 | Key Parameters of Flexible Tactile Sensors

The practical performance of flexible tactile sensors hinges on the synergistic optimization of their core parameters. Sensitivity, as the fundamental metric, determines the device's ability to detect subtle forces, forming the cornerstone of sensing precision. Broad linear range ensures stable signal output across diverse scenarios, from gentle touches to intense compressions, addressing the inherent trade-off between high sensitivity and wide detection limits. Meanwhile, parameters



such as response speed, long-term stability, and noise immunity, though often overlooked, are critical for dynamic signal capture, device durability, and environmental adaptability. This section systematically examines optimization strategies and recent advances in sensitivity, linearity, and other key parameters, offering theoretical insights and technical pathways for designing high-performance flexible tactile sensors.

### 2.3.1 | Sensitivity

Sensitivity, defined as the ratio of output electrical signal variation to input mechanical force change, is a critical metric for evaluating the precision and responsiveness of flexible tactile sensors. High sensitivity enables fine discrimination of subtle stimuli, enhancing robotic tactile perception and human-machine interaction (HMI) safety. Current research focuses on improving sensitivity through advanced materials and microstructural designs [100–103]. Microstructures such as pores, pillars, pyramids, hemispheres, and random patterns are widely explored to amplify pressure-induced resistance changes [104].

For instance, Liu et al. [105] developed an interconnected porous elastic sensing layer via phase inversion and sacrificial templating. Using a ternary system (thermoplastic polyurethane (TPU), N, N-dimethylformamide (DMF), and water) with silver nanowires and soluble NaCl particles, they achieved a porous TPU layer with a low compressive modulus (23.8 Pa). The resulting pressure sensor exhibited ultrahigh sensitivity ( $1167 \text{ kPa}^{-1}$  within 1179 Pa) and a detection limit of 1.34 Pa (Figure 4a). Zhao et al. [109] combined CNT networks with hydrogel micropillar arrays, where pressure-induced interfacial contact area changes and 3D CNT percolation enabled a sensitivity of  $1050 \text{ kPa}^{-1}$  across 0.03–28 kPa, suitable for detecting acoustic waves and physiological signals. Li et al. [106] bioinspired by feline tongue papillae, designed a sensor with  $504.5 \text{ kPa}^{-1}$  sensitivity, 30 Pa–350 kPa range, and >8000-cycle stability, where stress redistribution across papillae enhanced performance (Figure 4b). Chen et al. [107] leveraged pyramid-shaped carbon foam and elastic spacers to achieve  $24.6 \text{ kPa}^{-1}$  sensitivity over 1.4 MPa, attributed to synergistic nonlinear piezoresistance and stiffness modulation (Figure 4c).

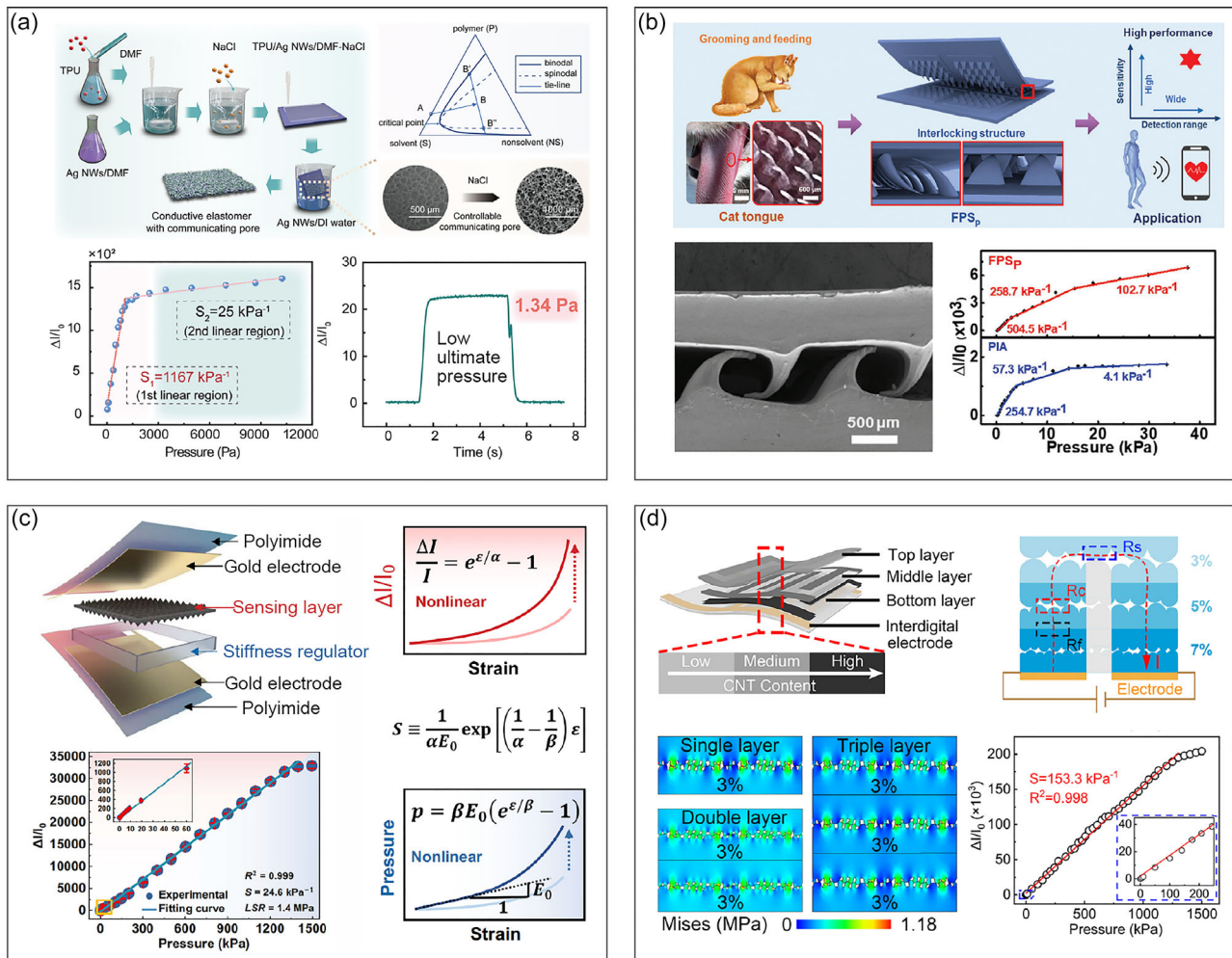


**FIGURE 4** | Key parameters of flexible tactile sensors. (a) Porous TPU active layer with ultrahigh sensitivity. Reproduced with permission [105]. Copyright 2024, John Wiley and Sons. (b) Feline tongue papillae inspired active layer with high sensitivity. Reproduced with permission [106]. Copyright 2024, John Wiley and Sons. (c) Pyramid-shaped carbon foam with high sensitivity and wide detection range. Reproduced under terms of the CC-BY license [107]. Copyright 2023, Springer Nature. (d) Multigradient sensor with high sensitivity and wide detection range. Reproduced with permission [108]. Copyright 2023, American Chemical Society.

### 2.3.2 | Broad Linear Range

For applications in general HMI and wearable devices, the required pressure range typically falls within 10 kPa. However, high-intensity wearable sports monitoring (e.g. jump detection) may demand sensors with an operational range of up to 500 kPa or even higher, necessitating the use of pressure sensors with a broad detection range [110]. A broad linear range ensures reliable detection across varying pressure levels, addressing the trade-off between high sensitivity and narrow detection limits. Multilayer or hierarchical microstructures are promising strategies to reconcile these demands [111–114].

Chen et al. [108] engineered a multigradient interdigital sensor with modulus, conductivity, and microstructure gradients, achieving  $153.3 \text{ kPa}^{-1}$  sensitivity over a wide range of 0.0005–1300 kPa (Figure 4d). Baek et al. [115] utilized 3D-printed hierarchical hemispheres to linearly increase electrode contact area, achieving  $162.5 \text{ kPa}^{-1}$  sensitivity across 0.05–300 kPa. Finite element analysis (FEA) confirmed deformability as the key to linearity. Li et al. [116] designed a multilayer nanofiber composite with sequential current path activation, broadening the linear range to 0–80 kPa. Wu et al. [117] employed gradient hemispheres to segment stress distribution, achieving a broad range of 0–600 kPa with a record linearity ( $R^2 = 0.99994$ ). Han et al. [118] integrated spine-like and porous microstructures with MXene/Ag and CNT/graphene networks, yielding  $3987 \text{ kPa}^{-1}$  sensitivity and 0–320 kPa range. He et al. [110] mimicked dogtail grass using ZnO nanowire-TPU interlocking structures, achieving  $29.7 \text{ kPa}^{-1}$  sensitivity and 0–2250 kPa broad range through uniform contact area expansion under pressure.

### 2.3.3 | Other Key Parameters

**2.3.3.1 | Response Time and Hysteresis.** Response time and hysteresis constitute critical parameters for flexible force sensors. Excessive response time can lead to signal distortion, thereby degrading sensor accuracy. Researchers typically optimize these characteristics through material selection and device structural design. For instance, Guo's group conducted a series of studies in this area [119–121]. They attribute hysteresis to gaps between electrodes and the viscoelastic medium layer, resulting in high energy dissipation. This prolonged duration limits the sensor's effectiveness in detecting high-frequency signals. To address this limitation, they incorporated 2 wt% CNTs into the PDMS dielectric to reduce its viscosity. Furthermore, they engineered bonding between microstructured microdomes and electrodes, effectively reducing the response relaxation time to approximately 0.04 ms.

**2.3.3.2 | Stability and Conformability.** Conformal deformation to attached surfaces poses a critical challenge to sensor accuracy and operational lifespan, representing one of the key factors affecting performance. To address this issue, researchers commonly employ strategies that control in-plane stress-strain distribution to enhance sensor stability. These include designing island-bridge structures, kirigami/origami configurations, and wrinkled architectures [87, 122]. For instance, Zhang et al. [123] demonstrated the use of photoreticulated strain-localizing membranes (prslPDMS) to fabricate ultralow-crosstalk sensor arrays. These arrays form microcage structures, reducing pixel overflow deformation by 90.3% compared to conventional flexible electronics. Notably, prslPDMS

functions both as an adhesive layer and an isolation barrier for pressure sensing. Consequently, the sensors achieve sufficient pressure resolution to detect weights as low as 1 g even under bending conditions, enabling clear pressure imaging and ultralow crosstalk (−33.41 dB) without complex data processing. This positions them as promising candidates for precision tactile detection. Separately, Sun et al. [124] proposed a strategy to mitigate strain concentration induced by rigid islands in stretchable electronics, guided by finite element simulations and validated through structural design and experiments. Their method utilizes graded-transparency masks to create gradient-modulus regions between photopolymerized rigid islands and soft substrates. This approach alleviates strain concentration at interfaces caused by modulus discontinuity by spatially expanding the scale of modulus variation. Thereby, it prevents premature substrate failure resulting from localized strain constraints during stretching.

**2.3.3.3 | Noise Immunity.** Capacitive sensors are highly susceptible to external interference, which severely limits their application scope. Although numerous studies have focused on improving the SNR of capacitive sensors, most approaches concentrate on designing shielding layers [125] to reduce noise. This strategy inevitably complicates sensor architecture. Recently, alternative solutions have emerged that enhance SNR without altering the primary sensor structure by amplifying capacitive signals [126]. Han et al. [127] developed a ternary composite film by hybridizing PVDF with core-shell AgNWs@TiO<sub>2</sub> nanostructures. This design yielded a wearable flexible capacitive pressure sensor exhibiting high dielectric constant and exceptional SNR (interference resistance). The sensor's superior anti-interference performance stems primarily from the core-shell structure, which increases the dielectric constant, elevates initial capacitance, and ultimately amplifies SNR. Validated through a smart glove sensing system, this sensor maintains high SNR against various interference sources, providing a new paradigm for developing highly interference-resistant capacitive flexible pressure sensors. Building on this foundation, Xu et al. [128] likewise achieved SNR enhancement in capacitive flexible force sensors by utilizing liquid metal hybrid fibers.

## 3 | Intelligent Algorithms Applied to Tactile Sensors

Intelligent algorithms provide systematic solutions for enhancing multidimensional performance and enabling complex-scenario applications of tactile sensors. Here, we first provide a brief primer on the fundamental concepts of AI algorithms. Following this foundation, we successively explore their transformative applications in four critical areas: enhancing tactile sensor performance, advancing pattern recognition capabilities, achieving multimodal data fusion, and empowering intelligent closed-loop control.

### 3.1 | Introduction of Intelligent Algorithms

AI, particularly ML, has become a foundational technology for advancing flexible sensing systems, enabling transformative



capabilities in data processing, pattern recognition, and intelligent decision-making [129, 130]. By learning directly from data, ML algorithms bypass the need for explicit physical or mathematical modeling, making them especially suited for handling complex, multidimensional signals generated by flexible sensors in dynamic environments [15, 16].

ML is broadly categorized into supervised, unsupervised, and reinforcement learning. Supervised learning relies on labeled datasets to train models for classification and regression tasks. Unsupervised learning techniques such as clustering and dimensionality reduction are invaluable for discovering hidden patterns in sensor data without preexisting labels. Reinforcement learning, though less commonly employed in sensory applications, offers potential in adaptive systems where sensors interact with environments, such as in embodied robotics.

Classical algorithms, including support vector machines (SVM) and artificial neural networks (ANN), provide powerful tools for classification tasks such as gesture recognition and physiological monitoring. SVM effectively constructs optimal decision

boundaries in high-dimensional spaces, while ANN mimics biological neural networks to handle complex nonlinear relationships in sensor data [131–133].

DL architectures further enhance processing capabilities for sophisticated sensing applications. Convolutional neural networks (CNN) excel at extracting spatial features from sensor array data, making them invaluable for tactile pattern recognition [134]. Recurrent neural networks (RNN) and their variants specialize in analyzing time-series data from dynamic sensor readings, enabling real-time activity recognition and predictive modeling [135].

Besides, dimensionality reduction methods such as principal component analysis (PCA) and t-distributed stochastic neighbor embedding enable effective visualization and processing of high-dimensional sensor information, while clustering algorithms like k-means facilitate pattern discovery and anomaly detection without preexisting labels [136]. These approaches are particularly valuable for exploratory data analysis and feature extraction in complex sensing environments.

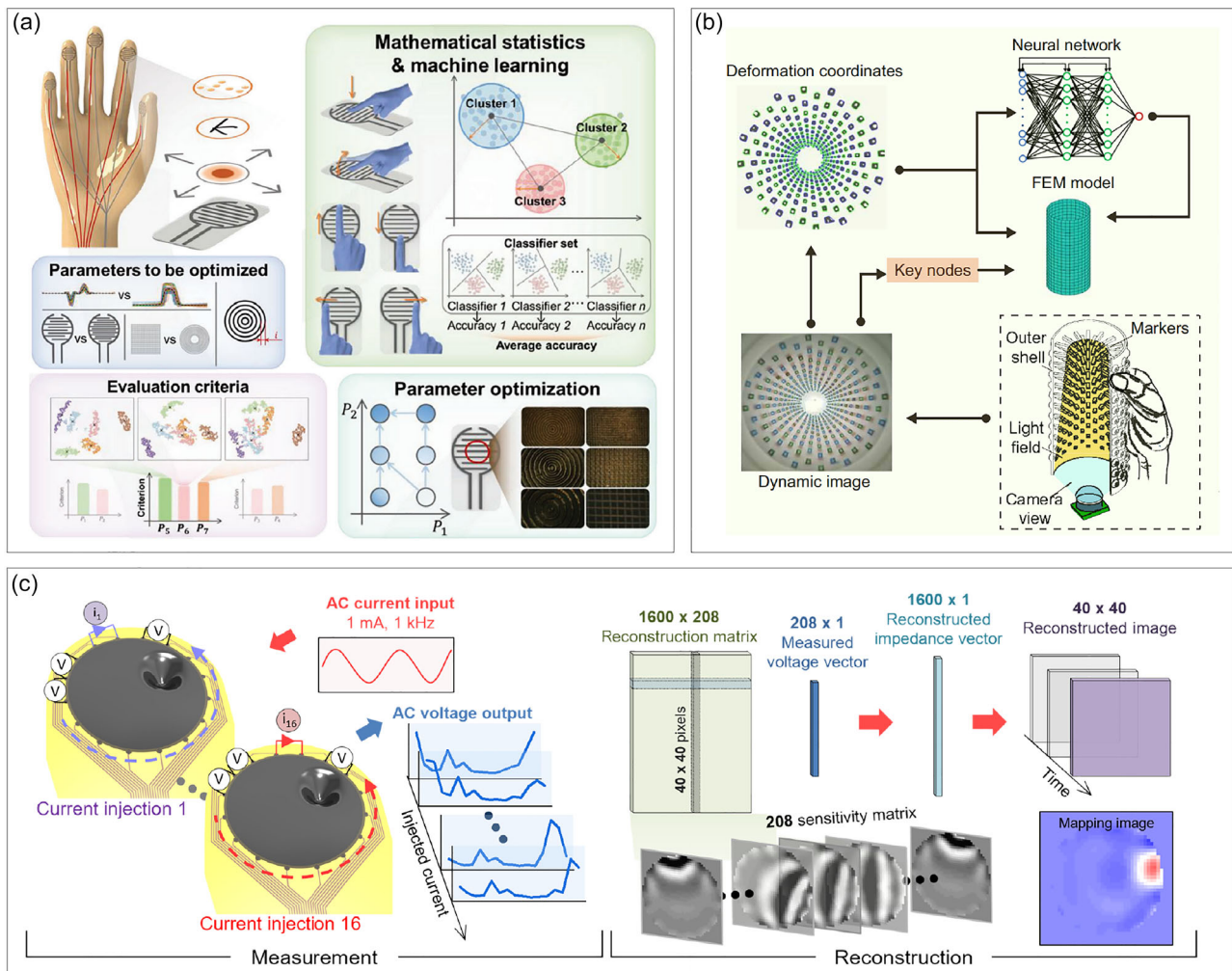


**FIGURE 5** | AI-driven performance optimization of sensors. (a) ML-based parameter tuning and optimization. Reproduced under terms of the CC-BY license [23]. Copyright 2023, John Wiley and Sons. (b) PINNs-based force reconstruction. Reproduced under terms of the CC-BY license [138]. Copyright 2025, The American Association for the Advancement of Science. (c) Neural network algorithms parameterize multimodal pressure signals. Reproduced under terms of the CC-BY license [139]. Copyright 2024, The American Association for the Advancement of Science.

### 3.2 | AI-Driven Performance Optimization of Sensors

Intelligent methodologies have established innovative pathways for advancing pressure sensor performance and systematic modeling. Traditional parameter optimization, reliant on empirical trial-and-error or finite element simulations, grapples with high computational costs and poor multiobjective coordination. ML and DL techniques, however, enable data-driven decoding of sensor input–output correlations, accelerating the paradigm shift from empirical design to intelligent design. Meanwhile, digital model construction remains constrained by nonlinearities in sensing mechanisms and nonintuitive stimulus–response mappings. The integration of ML not only reveals latent relationships within these complexities but also enhances data decoupling capabilities, ultimately refining sensor performance.

#### 3.2.1 | Parameter Tuning and Optimization

ML and reinforcement learning facilitate adaptive sensor parameter adjustments, dynamically optimizing measurement states under environmental variations to enhance system performance [137]. As illustrated in Figure 5a, Lu et al. [23] developed an ML-guided flexible tactile sensor system achieving  $\approx 99.58\%$  classification accuracy across six dynamic touch modes. Diverging from intuition-driven designs, this approach employs SVM-based ML algorithms and statistical criteria for manufacturing parameter selection, uncovering latent features in raw sensor data. For user-specific optimization, Luo et al. [140] designed a digitally embroidered smart glove integrating tactile sensors and vibrotactile actuators, enabling adaptive haptic feedback tuning for diverse user behaviors through ML algorithms.

#### 3.2.2 | Data-Driven Modeling

AI-driven inference architectures establish complex mappings between pressure/tactile data and physical motions, extracting patterns to characterize model feature vectors and parameters, thereby enabling “data-to-model” construction. In Figure 5b, Tang et al. [138] mimicked the helical microstructure of aloe vera leaves to design a 3D spiral tactile sensor with dual-color markers. By integrating physics-informed neural networks (PINNs), they achieved high-precision force reconstruction (relative error  $< 2.3\%$  within 0.5–25 N), supporting applications in tennis swing analysis, virtual reality (VR) object manipulation, and robotic grasping. Kim et al. [139] eliminated traditional complex wiring by developing an ultrathin electrical impedance tomography-based electronic skin (Figure 5c) with sparse edge sensing points. Neural network algorithms parameterize multimodal pressure signals (multipoint contact, intensity, location), achieving 1.7 pixels/mm spatial resolution and submillimeter pressure sensitivity for reliable human–robot interaction. Kong et al. [141] introduced a DL algorithm called the self-attention-assisted tactile super-resolution (SR) model, which enables SR pressure detection by dynamically generating vast virtual taxels from only 23 physical units, achieving a high spatial resolution. Data-driven frameworks also enable 3D force perception. Iskandar et al. [142] realized intrinsic tactile sensing in robotic arms without artificial skin by combining multivariate learning and ANN to reconstruct externally applied 3D forces via high-resolution joint torque sensing.

### 3.3 | AI-Driven Pattern Recognition and Perception

Tactile sensors generate distinct response signals under varied external stimuli, enabling AI algorithms to achieve advanced pattern recognition and perception, particularly in posture analysis and object identification.

#### 3.3.1 | Posture Perception

Wearable flexible pressure sensors exhibit unique response characteristics during human motions. Leveraging intelligent training and feature extraction of sensor data enables accurate recognition of gestures, postures, and gait patterns. Beigh et al. [143] designed a 36-channel plantar pressure sensor array (Figure 6a) and trained a 2D CNN model to classify four gait patterns (standing, walking, running, jumping) with 98.5% accuracy. Potluri et al. [145] integrated inertial measurement units with plantar sensors, employing PCA for dimensionality reduction and SVM-ANN hybrid learning to achieve 87.08% accuracy in multiphase gait classification, supporting clinical gait analysis for movement disorders.

#### 3.3.2 | Object Identification through Softness Detection

Softness detection is a critical capability for robotic manipulation, enabling robots to distinguish objects by their mechanical compliance. This is achieved through active tactile exploration using controlled tapping or sliding motions. During these actions, the pressure-deformation relationship is analyzed to differentiate compliant from rigid objects. The resulting sensor data captures essential information about an object’s elastic properties and viscoelastic responses under various contact conditions [146, 147].

Advanced AI algorithms, particularly DL architectures, play an essential role in decoding the complex spatiotemporal patterns embedded in the sensor data during these interactions. Lee et al. [148] developed a tactile sensor to extract deformation time during the transient indentation process. This data, processed by a 1D-CNN algorithm, achieved 100% accuracy in distinguishing material softness. Lin et al. [146] developed a customized SVM that incorporates material softness and compliance recognition, significantly enhancing identification accuracy. As shown in Figure 6b, Chen et al. [30] created a neuromorphic tactile system encoding dynamic tactile information via millisecond-level spiking signals. The temporal dynamics of tactile signals provide crucial information about material compliance through precise spike timing patterns. These computational models enable real-time classification of object softness with high accuracy.

#### 3.3.3 | Comprehensive Object Identification

AI algorithms decode tactile signals during object contact or sliding for material and shape recognition [26, 146, 149–151]. While vertical pressure enables the softness detection, sliding touch allows for the assessment of surface texture, enabling comprehensive object recognition. The technological foundation for texture detection typically involves spectral analysis of high-frequency vibrations generated during sliding contact between the sensor and material surface. These vibrational signatures contain distinctive frequency components and temporal patterns that are characteristic of specific material properties and surface

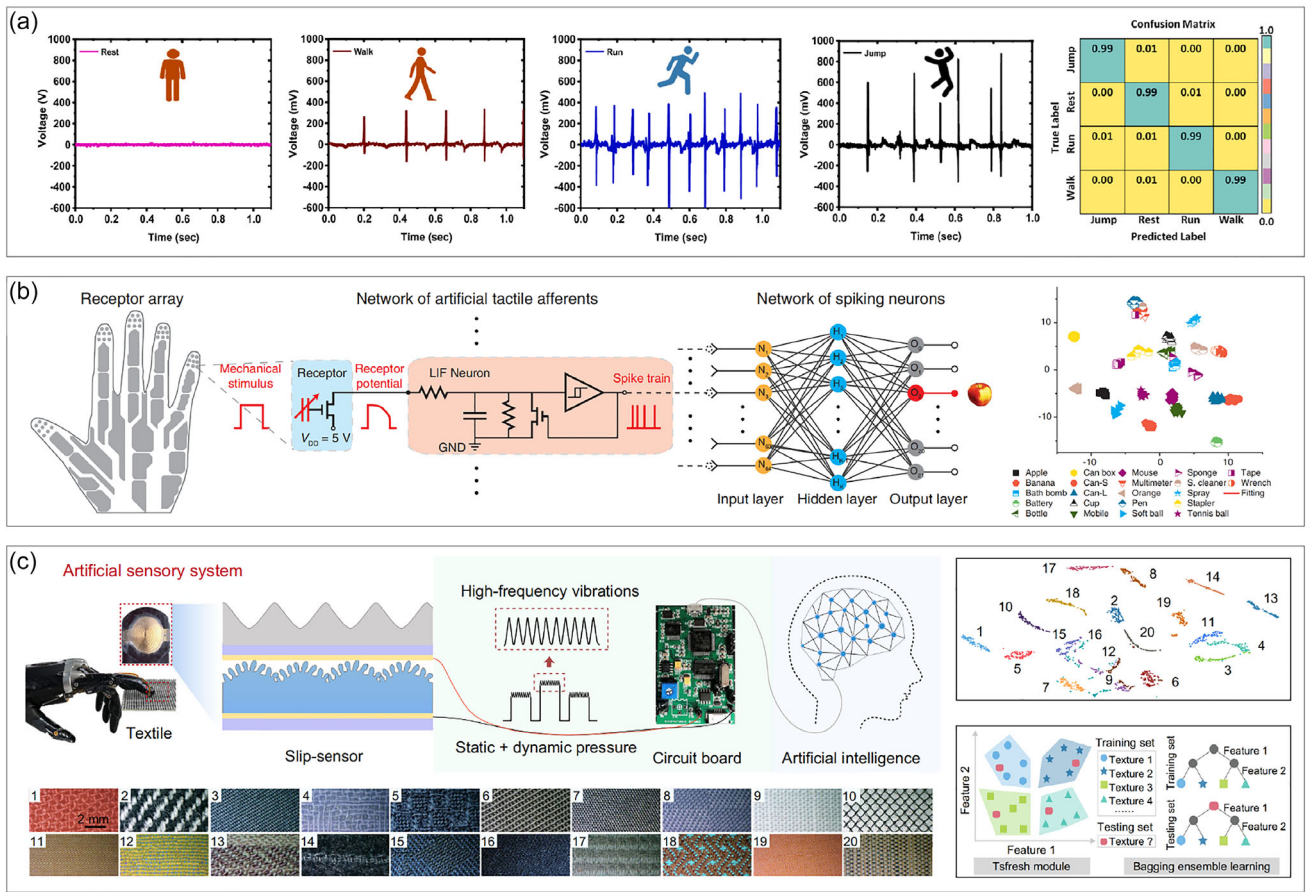


**FIGURE 6** | AI-driven pattern recognition and perception. (a) 2D CNN model-based gait recognition. Reproduced with permission [143]. Copyright 2023, Elsevier. (b) Spike timing-based coding for object classification. Reproduced with permission [30]. Copyright 2024, The American Association for the Advancement of Science. (c) ML-based sliding waveform analysis for texture recognition. Reproduced under terms of the CC-BY license [144]. Copyright 2023, Springer Nature.

textures. Bai et al. [144] engineered surface microstructures to generate material-specific vibration frequencies during sliding, achieving 98.9% identification accuracy under random sliding speeds using ML-based waveform analysis (Figure 6c). Shi et al. [134] developed a self-powered triboelectric floor mat with CNN-driven object recognition (96% accuracy). Sundaram et al. [152] designed a scalable tactile glove with 548 piezoresistive sensors, processing 135 000 object interaction frames via CNN to attain 96% object recognition accuracy and weight prediction (error < 57 g). Chen et al. [153] implemented a hydrogel-based tactile system on robotic fingers, combining iterative grasping with ML to achieve 100% accuracy in basic shape recognition.

### 3.4 | Multimodal Data Processing and Fusion

Multimodal fusion in flexible tactile sensing encompasses both the integration of tactile sensors with different transduction mechanisms (e.g., capacitive, resistive) and the synergy between tactile sensors and heterogeneous modalities like vision or temperature. The former enhances measurement fidelity through multidimensional tactile signal integration, while the latter supports complex applications in robotics, biomechanics, and medical diagnostics.

#### 3.4.1 | Multimodal Tactile Fusion for Enhanced Performance

Multimodal tactile sensors capture diverse tactile dimensions (e.g., high-/low-frequency signals), while AI algorithms fuse these signals to improve perception. Qiu et al. [154] developed a bioinspired dual-mode sensor combining piezoelectric dynamic hardness detection and piezoresistive static texture measurement. Leveraging CNN-based spectral analysis, they achieved 92.17% texture recognition accuracy, with FEA-deep neural networks synergy reducing friction coefficient errors below 10%. Hong et al. [155] engineered an artificial synaptic mechanoreceptor array integrating triboelectric sensing and ion-gel-gated rGO synaptic transistors. By fusing slow-adapting (SA) and fast-adapting (FA) mechanoreceptors with optimized algorithms, they enhanced data efficiency and recognition precision (Figure 7a). Han et al. [158] mimicked human fingerprints using triboelectric microneedle arrays and ResNet50, achieving 98.33% material classification accuracy for cost-effective robotic tactile systems.

#### 3.4.2 | Multimodal Synergy in Complex Scenarios

The intelligent fusion of tactile sensing with heterogeneous sensors (such as temperature and vision) enables significantly refined recognition capabilities in challenging environments.



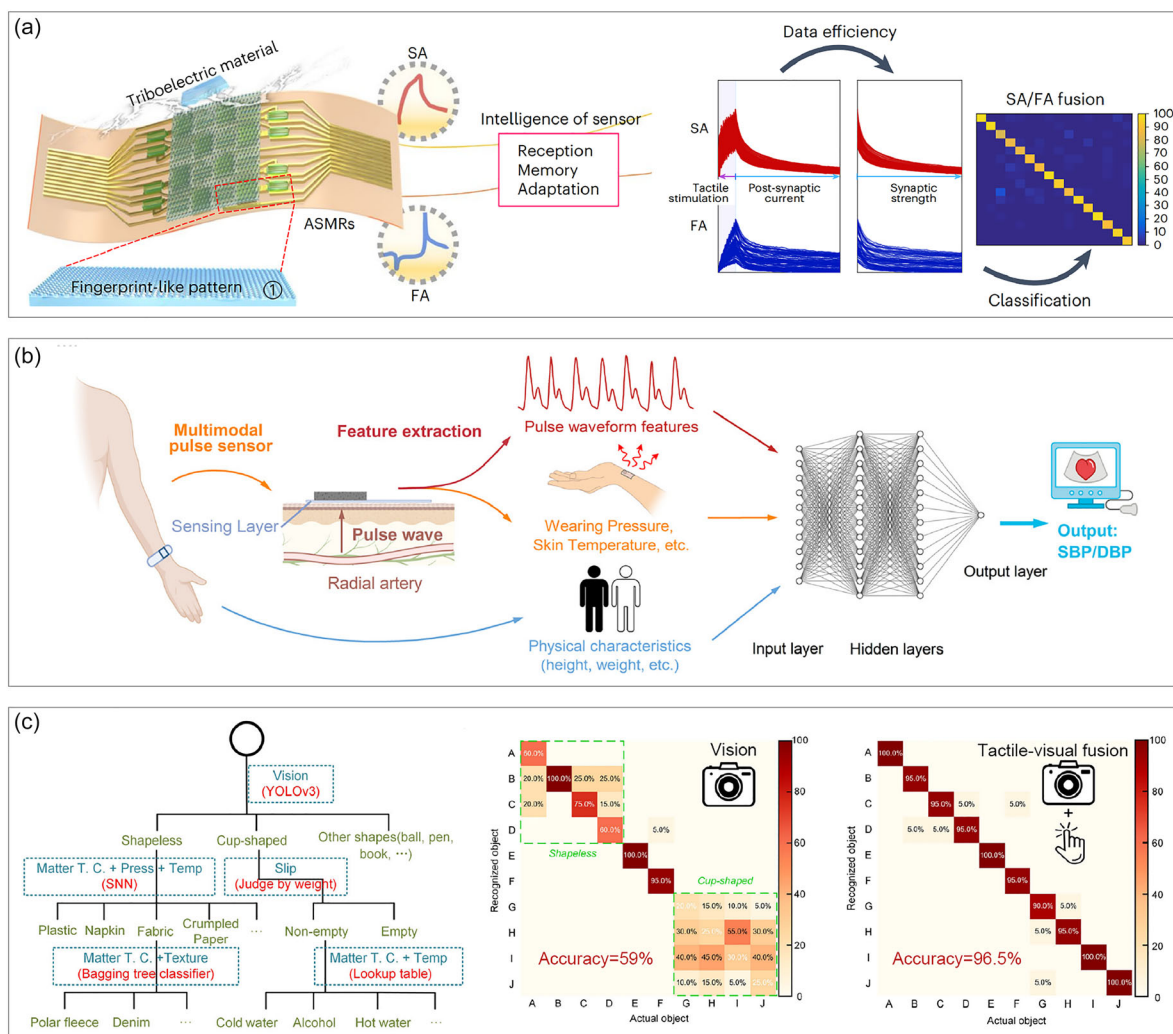


**FIGURE 7** | Multimodal data processing and fusion. (a) Enhancing data efficiency and recognition precision by fusing SA and FA mechanoreceptors with optimized algorithms. Reproduced with permission [155]. Copyright 2025, Springer Nature. (b) A piezoresistive-thermoelectric fusing sensor for accurate diagnosis. Reproduced under terms of the CC-BY license [156]. Copyright 2024, Royal Society of Chemistry. (c) Tactile-visual fusion algorithms enhancing recognition accuracy. Reproduced under terms of the CC-BY license [157]. Copyright 2024, Springer Nature.

This synergistic approach overcomes the limitations of unimodal sensing by compensating for signal ambiguity and environmental noise inherent in complex, dynamic scenarios. Tian et al. [156] designed a piezoresistive-thermoelectric blood pressure sensor that synchronously measures pulse waves, skin temperature, and wearing pressure, reducing systolic/diastolic pressure errors to 3.91 mmHg via ML (Figure 7b). Chen et al. [159] combined capacitive-resistive sensors to monitor respiratory airflow and temperature, using ML classifiers to achieve 95.6% accuracy in detecting physiological states (rest/activity/cough). Sun et al. [160] integrated triboelectric curvature/tactile sensors with pyroelectric PVDF temperature sensors in a soft robotic arm, attaining 97.14% accuracy in 28-class object recognition via 1D-CNN.

Tactile-visual fusion has gained prominence for complementary perception: vision mainly provides spatial localization, while tactile data enriches object classification [161, 162]. Suresh et al. [163] proposed NeuralFeels, a neural field framework achieving 4.7 mm average pose estimation drift via tactile-visual fusion. Mao et al. [157] combined tactile sensors with YOLOv3-CNN vision recognition, boosting classification accuracy from 59% (vision-only)

to 96.5% (Figure 7c). Jiang et al. [164] developed a 1152-channel tactile glove system reconstructing deformable object geometries with 97.6% force accuracy and 1.8 cm shape error. Liang et al. [165] fused radar-based hand motion tracking with wrist-worn pressure arrays via hierarchical SVM, improving differentiation of nuanced gestures (e.g., “tap” vs. “press”). Lee et al. [166] created a  $10 \times 10$  multifunctional array (strain/ pressure/bend/temperature) using Ag nanowire-CB/PDMS composites, classifying 45 hybrid stimuli via Bag-of-Words ML.

### 3.5 | Sensor-Intelligence-Actuator Closed-Loop System

The integration of flexible tactile sensors with intelligent algorithms enables not only perception and classification but also active interaction with the environment through closed-loop control [167, 168]. In advanced robotic and wearable systems, tactile data is processed by AI-driven inference engines (e.g., reinforcement learning agents or convolutional-decision networks), which generate real-time actuation commands [169–171]. These commands can be utilized

to adjust grasping force, modify prosthetic stiffness, or provide haptic feedback to users, forming a closed-loop system [172–174]. Such a control paradigm is crucial for applications like surgical robotics, prosthetic limbs, and adaptive exoskeletons, where high-precision, low-latency response is essential.

## 4 | Emerging Applications

Flexible tactile sensors, with their exceptional sensitivity, tunable mechanical properties, and environmental adaptability, are revolutionizing healthcare, HMI, and robotics. This chapter delineates their cutting-edge progress across three domains: wearable health monitoring, interactive devices, and robotic tactile systems.

### 4.1 | Wearable Health Monitoring

Flexible tactile sensors are driving the evolution of personalized, real-time, and intelligent healthcare technologies. Traditional

medical devices, constrained by rigid architectures, high costs, and operational complexity, fail to meet continuous monitoring requirements. Flexible sensors, leveraging miniaturized designs, high sensitivity, and conformal skin interfacing, enable real-time physiological signal acquisition, motion tracking, and assisted medical interventions [175, 176]. Integrated with ML algorithms, they further empower intelligent diagnostics and therapeutics.

#### 4.1.1 | Physiological Signal Monitoring

Flexible tactile sensors demonstrate significant applications in monitoring human physiological signals, particularly respiration, pulse, and blood pressure. Respiratory monitoring primarily employs two approaches: positioning sensors near the nasal/oral region to detect airflow forces during breathing [177–179], or attaching sensors to thoracic/abdominal areas to capture diaphragmatic movement-induced pressure variations [180]. Pulse signal detection is achieved by sensing subtle cutaneous pressure fluctuations from arterial pulsations, typically through sensor placement over radial [181, 182], digital [183], or carotid arteries [184]. Zeng et al. [178] developed a PEDOT:PSS-based

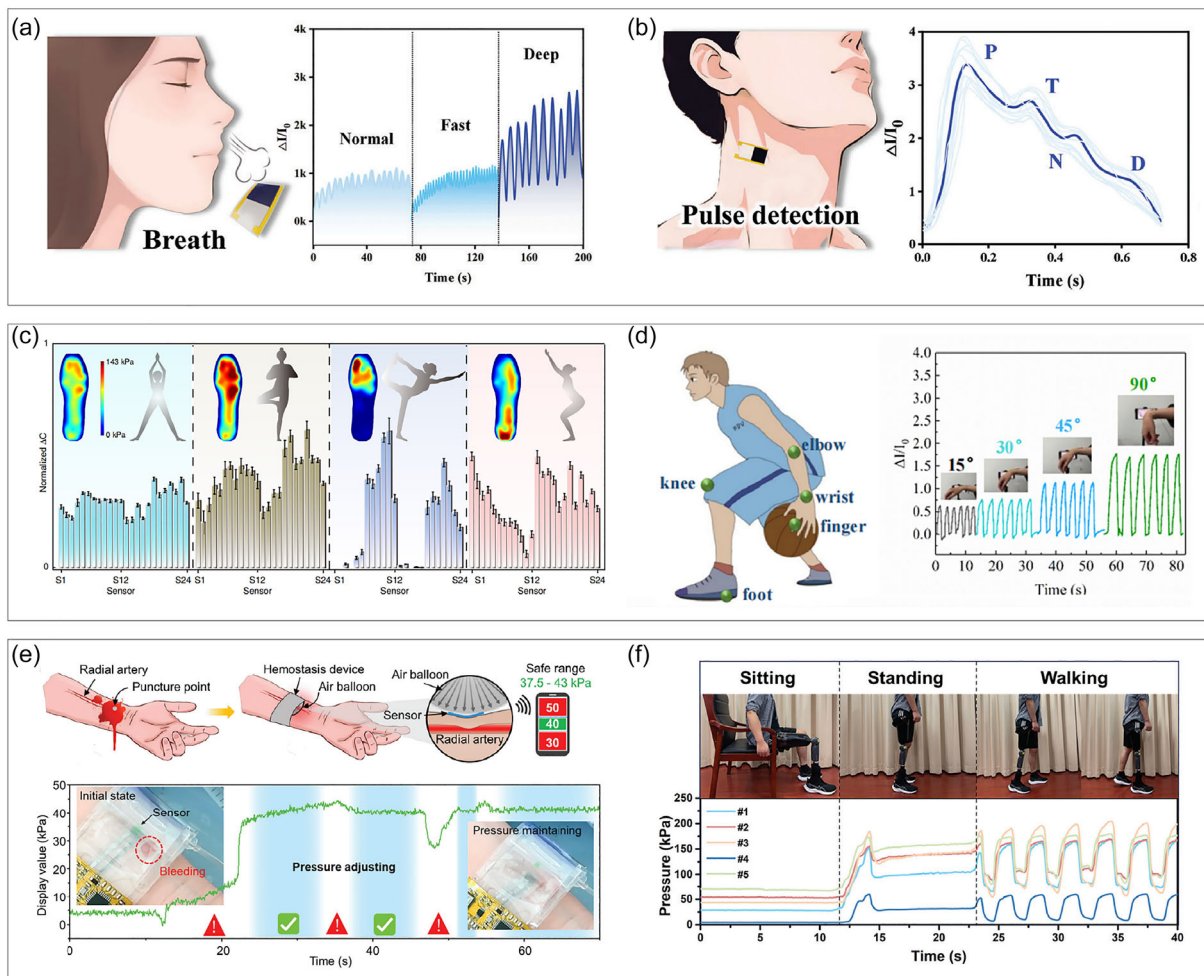


**FIGURE 8** | Wearable health monitoring. (a) Breath detection. (b) Pulse detection. Reproduced with permission [178]. Copyright 2024, John Wiley and Sons. (c) Gait detection. Reproduced under terms of the CC-BY license [28]. Copyright 2020, Springer Nature. (d) Sports posture detection. Reproduced with permission [185]. Copyright 2024, Royal Society of Chemistry. (e) Hemostatic medical device. Reproduced under terms of the CC-BY license [186]. Copyright 2023, John Wiley and Sons. (f) Prosthetic wear comfort assessment. Reproduced with permission [61]. Copyright 2024, John Wiley and Sons.

piezoresistive tactile sensor with high sensitivity ( $4 \times 10^5 \text{ kPa}^{-1}$  within 100 kPa range), enabling precise physiological monitoring. This device successfully detected respiratory frequency and amplitude during breathing assessment (Figure 8a) and captured carotid pulse waveforms when attached to neck skin (Figure 8b).

Integration with ML algorithms further enabled blood pressure estimation through pulse wave analysis [21, 181, 187, 188]. Wang et al. [189] designed an adaptive pressure wristband system mimicking traditional Chinese triple-finger diagnosis, utilizing a fully printed  $6 \times 9$  piezoresistive sensor array combined with ML models to predict cardiovascular health indicators from pulse waves. Their team also developed ML-based linear regression models for predicting systolic/diastolic blood pressure and mean arterial pressure through traditional pulse diagnosis patterns, advancing digitalized Chinese medicine. Fang et al. [190] created a waterproof textile-structured triboelectric sensor achieving continuous noninvasive blood pressure monitoring with supervised feedforward neural networks, maintaining systolic/diastolic pressure prediction errors within  $\pm 3\%$ .

Long-term monitoring of these signals allows intelligent algorithms to identify potential health risks including sleep apnea and cardiovascular abnormalities while providing personalized medical recommendations [31, 183]. The integration of multiuser flexible wearable systems shows promise for real-time group physiological monitoring in future smart elderly care facilities [191], combining multiparameter detection capabilities with enhanced diagnostic accuracy through ML and noninvasive continuous monitoring advantages.

#### 4.1.2 | Motion and Posture Analysis

The monitoring of human physiological signals offers early warning and diagnostic capabilities for potential health risks, while the detection of motion and posture provides health-conscious guidance for physical activities [12, 192]. Tactile sensors for movement and posture monitoring typically employ multiple discrete units distributed across body regions to detect localized pressure variations, thereby inferring whole-body positional changes [193–195]. Tao et al. [28] developed a smart insole incorporating 24 capacitive tactile sensors capable of real-time plantar pressure distribution analysis, enabling differentiation between standing postures and yoga poses (Figure 8c). Lu et al. [185] created a wide-range high-sensitivity piezoresistive sensor for joint motion tracking, demonstrating applicability in monitoring wrist flexion angles and similar articulations (Figure 8d).

Integration of sensing devices with intelligent algorithms enables biomechanical reconstruction for sophisticated motion/posture monitoring systems [196, 197]. Wang et al. [198] established a comprehensive rehabilitation assessment platform combining epidermal sensors with a multitask gait transformer to predict fall risks, evaluate walking capacity, and track recovery progress, achieving physician-level assessment consistency for intelligent rehabilitation management. Jiang et al. [199] devised a self-powered posture-monitoring vest using knitted dual-thread structures (nylon and conductive fibers) to capture real-time torso deformation signals. Their random forest algorithm achieved 96.6% accuracy in classifying six typical sitting postures

through cervical, thoracic, and lumbar signal analysis, providing preventive guidance for lumbar disorders. Liu et al. [200] implemented an active matrix sensing array for real-time plantar pressure monitoring, combined with a support vector machine to develop an AI diagnostic model distinguishing lumbar degenerative disease patients from healthy individuals.

These intelligent insoles and posture-monitoring devices not only enable scientific guidance for athletic training but also facilitate fall detection and alert systems for elderly individuals living alone [201, 202], advancing the development of smart exercise equipment and age-care technologies.

#### 4.1.3 | Medical Device Assistance

Flexible tactile sensors demonstrate promising applications in medical-assistive monitoring [203, 204], facilitating intelligent and personalized healthcare experiences. Zhang et al. [186] developed a wireless smart pressure sensing system based on capacitive tactile sensors, functioning as a hemostatic medical device (Figure 8e). This system monitors compression pressure during hemorrhage control and intelligently adapts pressure intensity according to individual patient characteristics, providing personalized and intuitive guidance for surgical hemostasis to enhance procedural quality. Yang et al. [61] proposed a high-performance capacitive sensor leveraging the Schottky effect for prosthetic wear comfort assessment (Figure 8f), enabling precise personalized medical recommendations for users.

Traditional standardized medical devices struggle to address biomechanical compatibility challenges arising from patient-specific variations. The integration of flexible tactile sensing systems with intelligent algorithms offers innovative solutions to this critical issue, paving the way for precise and individualized smart healthcare implementations.

### 4.2 | HMI

Flexible tactile sensors are revolutionizing human-machine interfaces by enabling natural, intuitive, and immersive interactions. Traditional interfaces relying on physical buttons and touchscreens constrain user experience flexibility and operational intuitiveness. The integration of flexible tactile sensing systems with intelligent algorithms enhances gesture recognition and voice interaction while unlocking transformative potential in VR and augmented reality (AR).

#### 4.2.1 | Intelligent Interactive Devices

Large-area tactile sensing arrays are a common type of gesture recognition device for HMI [205–207]. These arrays integrate multiple sensing units that can detect the trajectory and pressure information of a finger sliding across their surface [208]. Combined with intelligent algorithms for classification, they enable handwriting recognition applicable to touch interactions [209]. Inspired by the multiscale suckers of octopus tentacles, Chen et al. [210] designed a programable microdome tactile sensing array to monitor hand muscle activity. Using a random forest algorithm for real-time classification, they achieved 100% accuracy in recognizing different operation actions. Single-point



devices can also recognize handwriting based on pressure waveforms. Mimicking the hemispherical microstructures on rose petal surfaces, Chen et al. [211] developed an MXene/PDMS composite material for pressure sensors. By constructing a CNN-MobileNetv2 DL model, they achieved 87.77% accuracy in handwritten character recognition, enhancing the HMI capabilities of the electronic skin.

Beyond such classic handwriting recognition methods, Hou et al. [212] also proposed a novel oral tactile sensing pad enabling touchscreen-like control using the tongue and teeth (Figure 9a). By combining sensor data from the oral pad with RNN and CNN algorithms to classify touch semantics, this system enables interaction applications like typing, game control, and wheelchair navigation. The ultrasoft electronic skin developed by Kim et al. [139], mentioned in Section 3.1.2, achieves a spatial resolution of 1.7 pixels/mm and submillimeter pressure sensitivity. Incorporating neural network algorithms, their system was trained on the EMNIST dataset to recognize 26 letters. It can also be used for real-time drone control via touch input (Figure 9b).

Tactile sensors also find application in sound detection [29, 216–218]. Guo et al. [213] attached piezoresistive tactile sensors near the vocal cords on the neck to detect muscle vibration signals during speech. Employing DL algorithms for waveform recognition and classification, they achieved high-precision speech detection suitable for voice control applications (Figure 9c). Liu et al. [219] proposed a wireless flexible skin-attachable acoustic sensor. Using piezoelectric micromachined ultrasonic transducers and flexible electronics, it simultaneously captures laryngeal vibrations and skin movement. Leveraging a deep residual network, they significantly improved laryngeal speech feature classification, achieving 96.9% accuracy for phoneme classification and 99.5% for speaker recognition.

Flexible tactile sensors are also emerging in autonomous and assisted driving. Lu et al. [220] developed an intelligent takeover assistance system integrating triboelectric sensor gloves. Combining these with a time distributed CNN-long short term memory network model boosted behavior recognition accuracy to 94.72%, providing a real-time sensing solution for safe takeover in autonomous driving.

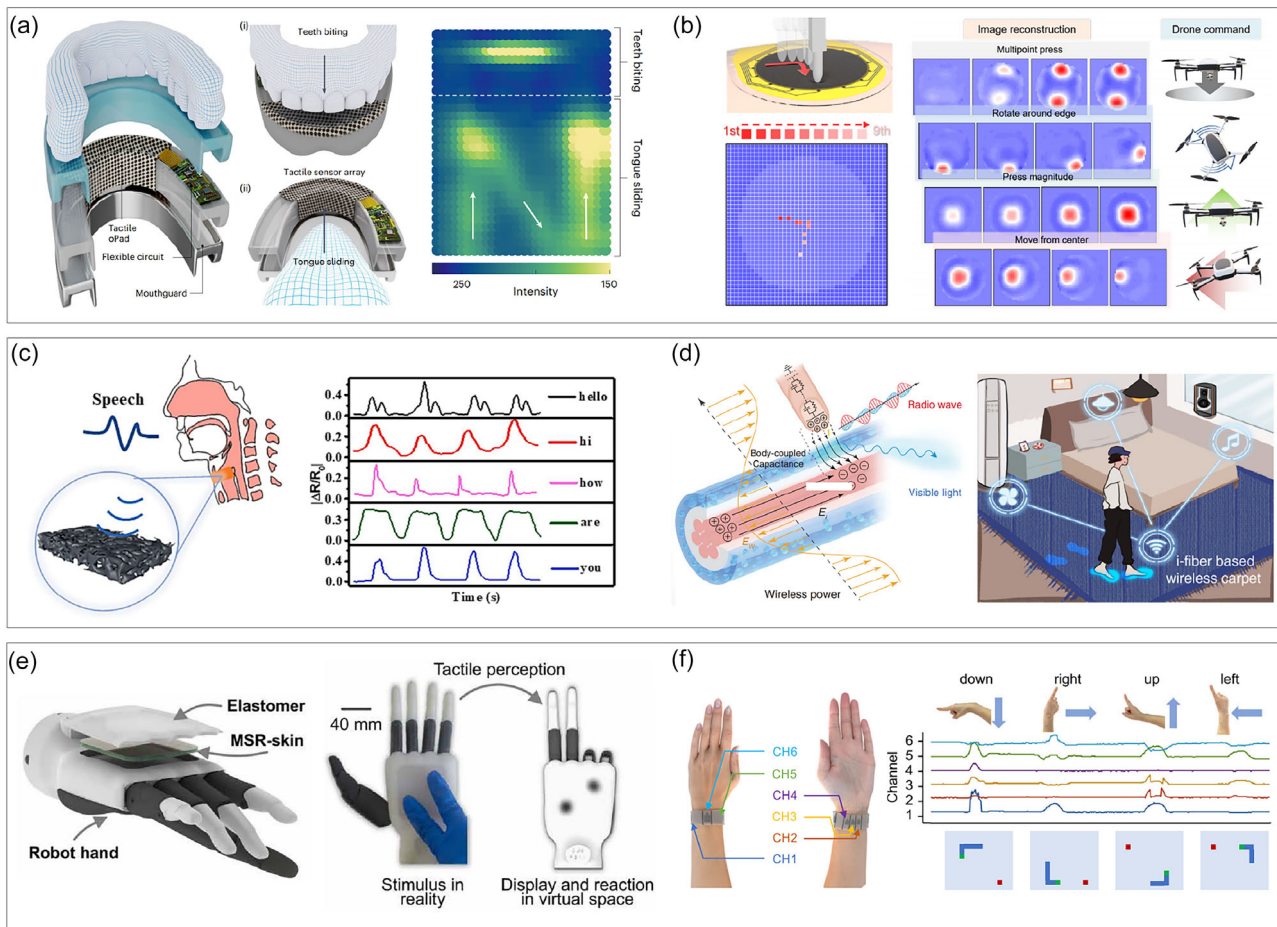


**FIGURE 9** | Human-machine interaction. (a) Oral tactile sensing pad for interaction applications. Reproduced with permission [212]. Copyright 2024, Springer Nature. (b) Tactile sensing pad for real-time drone control. Reproduced under terms of the CC-BY license [139]. Copyright 2024, The American Association for the Advancement of Science. (c) Tactile sensor for sound detection. Reproduced with permission [213]. Copyright 2024, Elsevier. (d) Chip-free wireless tactile sensor for smart home. Reproduced with permission [214]. Copyright 2024, The American Association for the Advancement of Science. (e) Robotic hand with a high-spatial-resolution tactile sensor array. Reproduced under terms of the CC-BY license [141]. Copyright 2025, The American Association for the Advancement of Science. (f) Tactile sensing system integrated into a wristband. Reproduced under terms of the CC-BY license [215]. Copyright 2025, Springer Nature.

To achieve chip-free interactive experiences, Yang et al. [214] designed smart tactile fibers capable of wireless visual-digital interaction. These fibers can perform signal sensing, visualization, and wireless transmission intrinsically, showing application potential in smart clothing and smart homes (Figure 9d).

Unlike traditional interactive mechanical buttons and wired circuits, HMI devices based on tactile sensing are moving toward multidimensional perception, multidevice collaboration, wireless operation, and intelligence through the deep integration of flexible electronics and AI.

#### 4.2.2 | VR/AR Integration

Tactile sensing-based interactive devices can also be applied in VR and AR fields [32, 221]. Tactile sensors capture real-world haptic properties through high-fidelity signal acquisition and

DL-driven feature extraction. This data is then used to construct accurate tactile perception models that enable realistic force and texture replication in AR/VR environments, enhancing immersive interaction [42, 222].

By equipping a robotic hand with a high-spatial-resolution tactile sensor array, Kong et al. achieved embodied tactile perception, paving the way for VR scene reconstruction (Figure 9e) [141]. Wen et al. [223] created self-powered triboelectric gloves for VR shooting interactions via ML-based pose reconstruction. Zhou et al. [224] developed a flexible pressure sensor using a composite nanofiber membrane. Combined with ML algorithms and integrated into a smart glove for sign language recognition, their system achieved 96.8% accuracy in letter recognition. Cheng et al. [215] proposed a thermally encapsulated capacitive tactile sensing system integrated into a wristband. Using a 1D-CNN algorithm, they achieved 96.63% accuracy in virtual

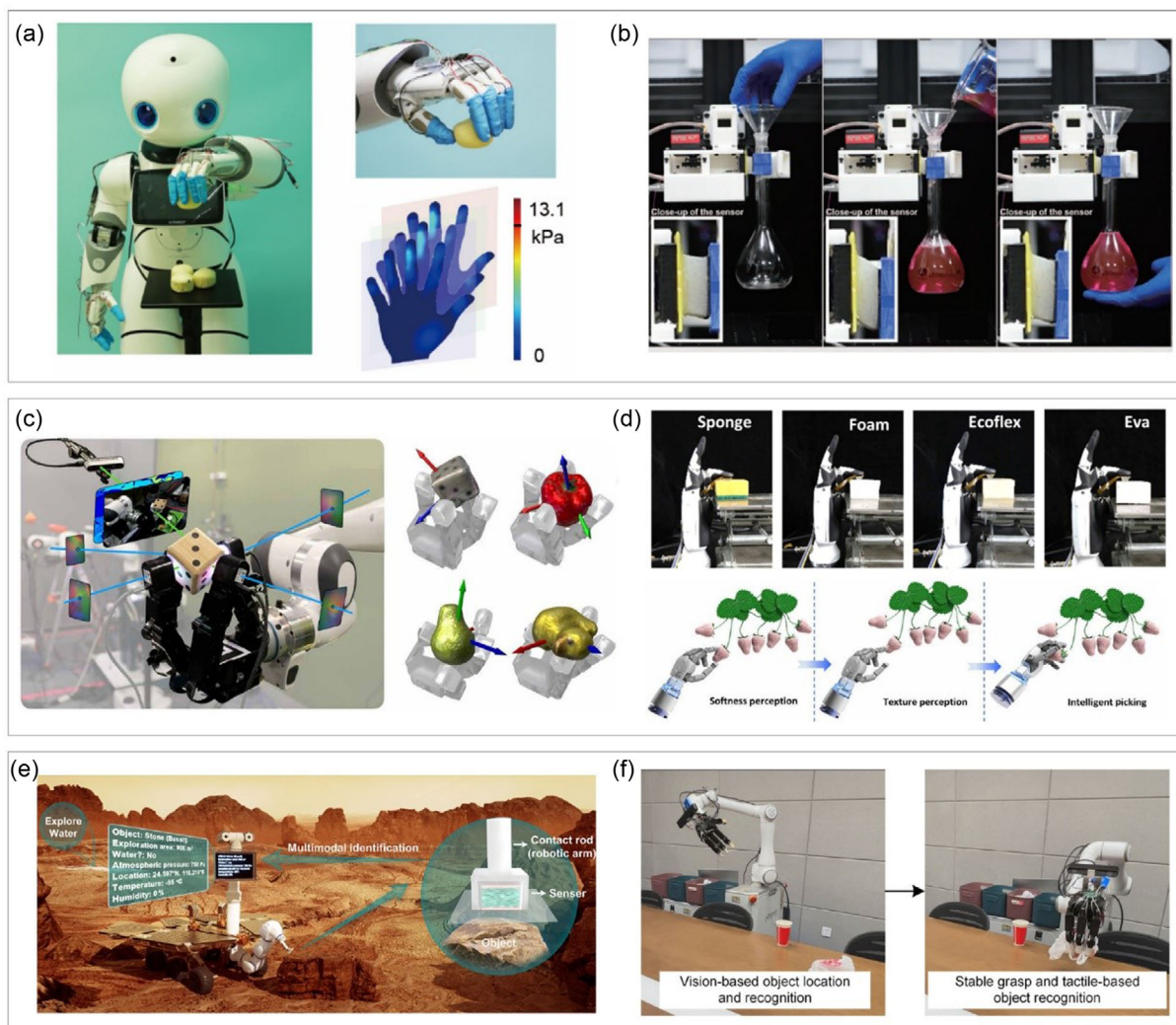


**FIGURE 10** | Applications of intelligent robotics. (a) Tactile feedback control for adaptive grip force adjustment. Reproduced with permission [27]. Copyright 2023, Elsevier. (b) Shear force detection for adaptive grip force adjustment. Reproduced with permission [229]. Copyright 2023, John Wiley and Sons. (c) Tactile-vision fusion for shape reconstruction and object recognition. Reproduced with permission [163]. Copyright 2024, The American Association for the Advancement of Science. (d) Tactile-vision fusion for texture recognition and intelligent farming picking. Reproduced under terms of the CC-BY license [154]. Copyright 2024, The American Association for the Advancement of Science. (e) Application for Mars exploration. Reproduced under terms of the CC-BY license [230]. Copyright 2023, Springer Nature. (f) Application for dexterous robotic housekeeping. Reproduced under terms of the CC-BY license [157]. Copyright 2024, Springer Nature.



handwriting recognition of letters, showing potential for VR games and AR recognitions (Figure 9f).

The synergy of tactile sensors, AI algorithms, and force feedback systems is redefining immersive experiences in virtual gaming, remote collaboration, and metaverse applications through multidimensional sensory integration [225–228].

### 4.3 | Intelligent Robotics

Tactile sensors are emerging as critical components for enabling precise manipulation and environmental cognition in intelligent robotics. Conventional robotic systems, constrained by preprogrammed operations, exhibit limited functional versatility and environmental adaptability. The integration of tactile sensing mechanisms with intelligent algorithms empowers robots with multimodal dexterity, enhanced situational awareness, and autonomous decision-making capabilities, driving transformative advancements in robotic intelligence.

#### 4.3.1 | Precision Manipulation

Robotic grasping of delicate or deformable objects (e.g., balloons, cakes) requires real-time force modulation to prevent damage. Bao et al. [27] addressed this challenge by integrating capacitive tactile sensors into humanoid robots (Figure 10a), creating a closed-loop system with signal acquisition, processing, and feedback control for adaptive grip force adjustment. Dai et al. [229] further advanced this capability using 3D tactile sensors to infer mass variations through shear force dynamics (Figure 10b), enabling continuous force optimization during variable-mass object manipulation. Such tactile feedback systems, coupled with intelligent control algorithms, demonstrate exceptional potential in medical robotics and precision manufacturing.

#### 4.3.2 | Environmental Cognition

The development of robot intelligence is further reflected in their environmental perception capabilities [231–233]. A common perception ability is the recognition of environments and objects [30, 144, 234, 235]. In typical robotic applications, visual perception is generally required for object localization. The various tactile algorithm strategies for object recognition introduced in Section 3.2 enable robots to achieve in-depth perception of environments and objects. Suresh et al. [163] combined visual and tactile perception on a multifingered hand to estimate the pose and shape of a grasped object, achieving shape reconstruction and object recognition during manipulation of novel objects (Figure 10c). The piezoelectric-piezoresistive dual-mode sensing sensor designed by Qiu et al. [154] applies to the recognition of various soft and hard objects and can be utilized in harvesting mature white strawberries where visual judgment is inadequate, facilitating the development of smart agriculture and intelligent harvesting (Figure 10d). Using touch to identify objects and materials effectively compensates for the shortcomings of visual object recognition. The multimodal tactile sensor designed by Zhao et al. [230] can perform object and environment recognition through ML, enabling the exploration and recognition of Martian terrain features with ultrahigh accuracy (Figure 10e). Mao et al. [157] reported a dexterous robotic hand featuring

multimodal tactile perception fused with vision, controlled by intelligent algorithms to achieve the entire process of object recognition, grasping, and sorted placement, laying the foundation for the development of intelligent home robotic assistants (Figure 10f).

With the enhancement of environmental perception capabilities through intelligent tactile sensing, intelligent robots are expected to transform from traditional single-task modes toward fully integrated, multisenario application models. Benefiting from iterative upgrades in sensor performance, continuous optimization of core algorithms, and the deep integration of multimodal perception technologies, the fields of smart prosthetics and humanoid robots are poised for breakthrough development opportunities.

## 5 | Challenges and Future Perspectives

### 5.1 | Technical Limitations

#### 5.1.1 | Challenges in the Integration of Flexible Tactile Sensors

While flexible pressure sensors have demonstrated exceptional laboratory performance, their real-world deployment in wearable systems faces critical barriers. Structural instability, including interfacial delamination during mechanical deformation and unreliable connections between sensors, conformal surfaces, and external circuits, remains a persistent challenge. These issues demand coordinated advancements in materials engineering and device architecture. Additionally, heterogeneous signal characteristics across sensor types (e.g., varying sensitivity ranges and nonlinear responses) complicate data acquisition and processing. Optimizing system-level performance requires concurrent innovations in sensor design and signal conditioning algorithms to ensure compatibility with diverse application requirements.

#### 5.1.2 | Algorithmic Complexity and Latency Constraints

State-of-the-art intelligent algorithms, particularly DL models, face a critical trade-off between computational complexity and real-time responsiveness. High-precision tactile perception tasks, such as dynamic gesture recognition, often suffer from latency due to the computational intensity of neural networks, which exceeds the tolerance threshold for seamless human–device interaction. Current research prioritizes three mitigation strategies: 1) developing lightweight neural architectures via model compression techniques like knowledge distillation; 2) adopting bioinspired event-driven paradigms such as spiking neural networks to reduce redundant computations; and 3) codesigning application-specific integrated circuits to enable edge computing with millisecond-level latency and microwatt-scale power consumption.

### 5.2 | Emerging Research Frontiers

#### 5.2.1 | Slip Perception Sensors

Slip detection represents an advanced stage of tactile sensing, involving the simultaneous measurement of shear forces and



surface sliding states under single-point contact [236]. Current research predominantly utilizes flexible pressure sensor arrays for indirect slip inference through contact trajectory analysis. For slip state identification, frequency-domain analysis of periodic deformation signals induced by frictional motion shows promise, requiring enhanced sensor sensitivity and optimized microstructures. For example, successful detection of object slip was achieved in the work of Liu et al. by monitoring high-frequency vibration signals using ultrahigh-sensitivity sensors [105]. Direct single-point slip detection and 3D shear force decoupling remain nascent but rapidly evolving areas [229, 237]. Shear force measurement strategies bifurcate into two approaches: 1) patterned electrode designs that exploit directional force distribution asymmetries, though limited by fabrication complexity for scalable arrays; and 2) strain centroid localization techniques, which demand sophisticated real-time signal processing enhanced by ML to improve accuracy and temporal resolution.

### 5.2.2 | Multimodal Sensor Fusion

Next-generation tactile systems will increasingly rely on synergistic interactions with vision, temperature, and inertial sensors to achieve robust environmental cognition. In industrial automation, hybrid tactile-visual systems enable robotic grippers to differentiate material properties (e.g., cardboard vs. plastic containers) while verifying spatial positions, reducing fragile item handling errors. Navigation aids for the visually impaired exemplify tactile-thermal-GPS fusion, where haptic feedback conveys directional cues and obstacle proximity. Key technological milestones include: 1) cross-modal data alignment through unified spatiotemporal registration protocols; 2) adaptive sensor weighting mechanisms that prioritize tactile inputs in vision-limited environments; and 3) privacy-preserving federated learning frameworks for medical rehabilitation devices to leverage multi-institutional tactile datasets without raw data sharing.

### 5.2.3 | Integrated System Miniaturization and Cost Reduction

The commercialization of tactile sensing hinges on overcoming miniaturization and cost barriers. Current flexible sensors suffer from interconnect reliability issues under cyclic bending, necessitating novel fabrication methods like roll-to-roll nanoimprinting to mass-produce durable, low-cost sensor arrays. Energy self-sufficiency is being addressed through hybrid triboelectric-piezoelectric energy harvesters that convert mechanical deformations into operational power. Chip-scale integration represents the ultimate goal, with emerging “lab-on-chip” designs combining sensing, processing, and wireless communication modules into submillimeter flexible electronics. For instance, heterogeneous integration of organic semiconductors and silicon-based circuits enables ultrathin flexible hybrid electronics capable of real-time pressure-temperature mapping, paving the way for imperceptible wearable health monitors and dexterous robotic manipulators.

### 5.2.4 | Hybrid Integration of Flexible Sensing Systems

Future intelligent tactile platforms will rely heavily on the heterogeneous integration of flexible sensors with rigid computing chips, wireless communication modules, and energy harvesting/

storage units. Overcoming the mechanical mismatch between soft and hard components remains a significant challenge. Techniques such as island-bridge structures, microkirigami, and liquid metal interconnects have been developed to ensure stretchable conductivity. Furthermore, roll-to-roll printing and laser sintering offer scalable routes for high-density, multifunctional hybrid electronics. This hybridization paves the way for wearable systems that are lightweight, imperceptible, and capable of performing real-time, edge-based tactile computation.

## 6 | Conclusion

Driven by rapid advancements in AI, the Internet of Medical Things, and robotics, wearable flexible pressure sensors have garnered increasing attention from researchers. This review systematically summarizes recent progress in three critical areas: 1) novel materials and structural designs for high-performance devices, 2) intelligent algorithms to enhance tactile sensing capabilities, and 3) emerging applications of flexible tactile sensors. Furthermore, it identifies persistent technical challenges, including interfacial instability, heterogeneous signal integration, and edge computing latency, while outlining future research priorities such as multimodal fusion architectures and chip-scale integration strategies. By integrating fundamental insights with application-oriented perspectives, this work provides a comprehensive reference framework to guide the development of next-generation flexible sensing systems characterized by enhanced performance, embedded intelligence, and cross-domain adaptability.

### Acknowledgements

The authors thank the support of National Natural Science Foundation of China (grant nos. 62422120, 52371202, 52192610, 52125205, 52250398, and 52203307), the Natural Science Foundation of Beijing (grant no. L223006), Shenzhen Science and Technology Program (grant no. KQTD20170810105439418), and the Fundamental Research Funds for the Central Universities.

### Conflicts of Interest

The authors declare no conflicts of interest.

### References

1. Y. Wang, X. Wu, D. Mei, L. Zhu, and J. Chen, “Flexible Tactile Sensor Array for Distributed Tactile Sensing and Slip Detection in Robotic Hand Grasping,” *Sensors and Actuators, A: Physical* 297 (2019): 111512, <https://doi.org/10.1016/j.sna.2019.07.036>.
2. M. Xu, Y. Gao, G. Yu, C. Lu, J. Tan, and F. Xuan, “Flexible Pressure Sensor Using Carbon Nanotube-Wrapped Polydimethylsiloxane Microspheres for Tactile Sensing,” *Sensors and Actuators, A: Physical* 284 (2018): 260–265, <https://doi.org/10.1016/j.sna.2018.10.040>.
3. S. Khan, W. Dang, L. Lorenzelli, and R. Dahiya, “Flexible Pressure Sensors Based on Screen-Printed P(VDF-TrFE) and P(VDF-TrFE)/MWCNTs,” *IEEE Transactions on Semiconductor Manufacturing* 28, no. 4 (2015): 486–493, <https://doi.org/10.1109/tsm.2015.2468053>.
4. F.-R. Fan, Z.-Q. Tian, and Z. Lin Wang, “Flexible Triboelectric Generator,” *Nano Energy* 1, no. 2 (2012): 328–334, <https://doi.org/10.1016/j.nanoen.2012.01.004>.

5. X. Jing, H. Li, H.-Y. Mi, et al., "Highly Transparent, Stretchable, and Rapid Self-Healing Polyvinyl Alcohol/Cellulose Nanofibril Hydrogel Sensors for Sensitive Pressure Sensing and Human Motion Detection," *Sensors and Actuators, B: Chemical* 295 (2019): 159–167, <https://doi.org/10.1016/j.snb.2019.05.082>.
6. Y. Wang, J. Chen, and D. Mei, "Recognition of Surface Texture with Wearable Tactile Sensor Array: A Pilot Study," *Sensors and Actuators, A: Physical* 307 (2020): 111972, <https://doi.org/10.1016/j.sna.2020.111972>.
7. R. Mao, W. Yao, A. Qadir, et al., "3-D Graphene Aerogel Sphere-Based Flexible Sensors for Healthcare Applications," *Sensors and Actuators, A: Physical* 312 (2020): 112144, <https://doi.org/10.1016/j.sna.2020.112144>.
8. Y. Wang, M. Chao, P. Wan, and L. Zhang, "A Wearable Breathable Pressure Sensor from Metal-Organic Framework Derived Nanocomposites for Highly Sensitive Broad-Range Healthcare Monitoring," *Nano Energy* 70 (2020): 104560, <https://doi.org/10.1016/j.nanoen.2020.104560>.
9. Y. Wu, I. Karakurt, L. Beker, et al., "Piezoresistive Stretchable Strain Sensors with Human Machine Interface Demonstrations," *Sensors and Actuators, A: Physical* 279 (2018): 46–52, <https://doi.org/10.1016/j.sna.2018.05.036>.
10. Q. Shi, Z. Zhang, T. Chen, and C. Lee, "Minimalist and Multi-Functional Human Machine Interface (HMI) Using a Flexible Wearable Triboelectric Patch," *Nano Energy* 62 (2019): 355–366, <https://doi.org/10.1016/j.nanoen.2019.05.033>.
11. A. Kumar, "Methods and Materials for Smart Manufacturing: Additive Manufacturing, Internet of Things, Flexible Sensors and Soft Robotics," *Manufacturing Letters* 15 (2018): 122–125, <https://doi.org/10.1016/j.mfglet.2017.12.014>.
12. Y. Zhang, M. Qiu, X. Zhang, et al., "Skin-Inspired High-Performance E-Skin With Interlocked Microridges for Intelligent Perception," *Advanced Functional Materials* 35, no. 1 (2024): 2412065, <https://doi.org/10.1002/adfm.202412065>.
13. A. Chortos, J. Liu, and Z. Bao, "Pursuing Prosthetic Electronic Skin," *Nature Materials* 15, no. 9 (2016): 937–950, <https://doi.org/10.1038/nmat4671>.
14. T. J. K. Buchner, S. Rogler, S. Weirich, et al., "Vision-Controlled Jetting for Composite Systems and Robots," *Nature* 623, no. 7987 (2023): 522–530, <https://doi.org/10.1038/s41586-023-06684-3>.
15. T. Sun, B. Feng, J. Huo, et al., "Artificial Intelligence Meets Flexible Sensors: Emerging Smart Flexible Sensing Systems Driven by Machine Learning and Artificial Synapses," *Nano-Micro Letters* 16, no. 1 (2023): 14, <https://doi.org/10.1007/s40820-023-01235-x>.
16. Y. Wang, M. L. Adam, Y. Zhao, et al., "Machine Learning-Enhanced Flexible Mechanical Sensing," *Nano-Micro Letters* 15, no. 1 (2023): 55, <https://doi.org/10.1007/s40820-023-01013-9>.
17. S. Dargan, M. Kumar, M. R. Ayyagari, and G. Kumar, "A Survey of Deep Learning and Its Applications: A New Paradigm to Machine Learning," *Archives of Computational Methods in Engineering* 27, no. 4 (2019): 1071–1092, <https://doi.org/10.1007/s11831-019-09344-w>.
18. W. Huang, X. Xia, C. Zhu, et al., "Memristive Artificial Synapses for Neuromorphic Computing," *Nano-Micro Letters* 13, no. 1 (2021): 85, <https://doi.org/10.1007/s40820-021-00618-2>.
19. S. Dutta, "An Overview on the Evolution and Adoption of Deep Learning Applications Used in the Industry," *WIREs Data Mining and Knowledge Discovery* 8, no. 4 (2018): e1257, <https://doi.org/10.1002/widm.1257>.
20. X. Xiao, J. Yin, J. Xu, T. Tat, and J. Chen, "Advances in Machine Learning for Wearable Sensors," *ACS Nano* 18, no. 34 (2024): 22734–22751, <https://doi.org/10.1021/acsnano.4c05851>.
21. S. Min, J. An, J. H. Lee, et al., "Wearable Blood Pressure Sensors for Cardiovascular Monitoring and Machine Learning Algorithms for Blood Pressure Estimation," *Nature Reviews Cardiology* 22, no. 9 (2025): 629–648, <https://doi.org/10.1038/s41569-025-01127-0>.
22. X. Jiang, R. Chen, and H. Zhu, "Recent Progress in Wearable Tactile Sensors Combined with Algorithms Based on Machine Learning and Signal Processing," *APL Materials* 9, no. 3 (2021): 030906, <https://doi.org/10.1063/5.0043842>.
23. Y. Lu, D. Kong, G. Yang, et al., "Machine Learning-Enabled Tactile Sensor Design for Dynamic Touch Decoding," *Advanced Science* 10, no. 32 (2023): e2303949, <https://doi.org/10.1002/advs.202303949>.
24. T. Zhang, M. Zhao, M. Zhai, et al., "Improving the Resolution of Flexible Large-Area Tactile Sensors through Machine-Learning Perception," *ACS Applied Materials & Interfaces* 16, no. 8 (2024): 11013–11025, <https://doi.org/10.1021/acsaami.3c17880>.
25. Z. Hu, L. Lin, W. Lin, et al., "Machine Learning for Tactile Perception: Advancements, Challenges, and Opportunities," *Advanced Intelligent Systems* 5, no. 7 (2023): 2200371, <https://doi.org/10.1002/aisy.202200371>.
26. X. Zheng, R. Zhang, B. Ding, et al., "A Bionic Textile Sensory System for Humanoid Robots Capable of Intelligent Texture Recognition," *Advanced Materials* 37, no. 32 (2025): e2417729, <https://doi.org/10.1002/adma.202417729>.
27. R. Bao, J. Tao, J. Zhao, M. Dong, J. Li, and C. Pan, "Integrated Intelligent Tactile System for a Humanoid Robot," *Science Bulletin* 68, no. 10 (2023): 1027–1037, <https://doi.org/10.1016/j.scib.2023.04.019>.
28. J. Tao, M. Dong, L. Li, et al., "Real-Time Pressure Mapping Smart Insole System Based on a Controllable Vertical Pore Dielectric Layer," *Microsystems & Nanoengineering* 6 (2020): 62, <https://doi.org/10.1038/s41378-020-0171-1>.
29. Y. Liu, H. Xu, M. Dong, et al., "Highly Sensitive Wearable Pressure Sensor Over a Wide Sensing Range Enabled by the Skin Surface-Like 3D Patterned Interwoven Structure," *Advanced Materials Technologies* 7, no. 12 (2022): 2200504, <https://doi.org/10.1002/admt.202200504>.
30. L. Chen, S. Karilanova, S. Chaki, et al., "Spike Timing-Based Coding in Neuromimetic Tactile System Enables Dynamic Object Classification," *Science* 384, no. 6696 (2024): 660–665, <https://doi.org/10.1126/science.adf3708>.
31. T. Liu, G. Y. Gou, F. Gao, et al., "Multichannel Flexible Pulse Perception Array for Intelligent Disease Diagnosis System," *ACS Nano* 17, no. 6 (2023): 5673–5685, <https://doi.org/10.1021/acsnano.2c11897>.
32. Z. Sun, M. Zhu, X. Shan, and C. Lee, "Augmented Tactile-Perception and Haptic-Feedback Rings as Human-Machine Interfaces Aiming for Immersive Interactions," *Nature Communications* 13, no. 1 (2022): 5224, <https://doi.org/10.1038/s41467-022-32745-8>.
33. W. Cheng, X. Wang, Z. Xiong, et al., "Frictionless Multiphasic Interface for Near-Ideal Aero-Elastic Pressure Sensing," *Nature Materials* 22, no. 11 (2023): 1352–1360, <https://doi.org/10.1038/s41563-023-01628-8>.
34. Y. Su, C. Chen, H. Pan, et al., "Muscle Fibers Inspired High-Performance Piezoelectric Textiles for Wearable Physiological Monitoring," *Advanced Functional Materials* 31, no. 19 (2021): 2010962, <https://doi.org/10.1002/adfm.202010962>.
35. H.-J. Qiu, W.-Z. Song, X.-X. Wang, et al., "A Calibration-Free Self-Powered Sensor for Vital Sign Monitoring and Finger Tap Communication Based on Wearable Triboelectric Nanogenerator," *Nano Energy* 58 (2019): 536–542, <https://doi.org/10.1016/j.nanoen.2019.01.069>.
36. M. Su, P. Li, X. Liu, D. Wei, and J. Yang, "Textile-Based Flexible Capacitive Pressure Sensors: A Review," *Nanomaterials* 12, no. 9 (2022): 1495, <https://doi.org/10.3390/nano12091495>.
37. Y. Huang, X. Fan, S. C. Chen, and N. Zhao, "Emerging Technologies of Flexible Pressure Sensors: Materials, Modeling, Devices, and Manufacturing," *Advanced Functional Materials* 29, no. 12 (2019): 1808509, <https://doi.org/10.1002/adfm.201808509>.

38. M. Hassan, G. Abbas, N. Li, et al., "Significance of Flexible Substrates for Wearable and Implantable Devices: Recent Advances and Perspectives," *Advanced Materials Technologies* 7, no. 3 (2021): 2100773, <https://doi.org/10.1002/admt.202100773>.
39. H. Li, Y. Ma, and Y. Huang, "Material Innovation and Mechanics Design for Substrates and Encapsulation of Flexible Electronics: A Review," *Materials Horizons* 8, no. 2 (2021): 383–400, <https://doi.org/10.1039/d0mh00483a>.
40. X. Pan, J. Li, Z. Xu, et al., "A High Stretchability Micro-Crack Tactile Sensor System Based on Strain-Isolation Substrate," *Materials Today Physics* 48 (2024): 101562, <https://doi.org/10.1016/j.mtphys.2024.101562>.
41. Z. Tan, H. Li, Y. Huang, et al., "Breathing-Effect Assisted Transferring Large-Area PEDOT: PSS to PDMS Substrate with Robust Adhesion for Stable Flexible Pressure Sensor," *Composites Part A: Applied Science and Manufacturing* 143 (2021): 106299, <https://doi.org/10.1016/j.compositesa.2021.106299>.
42. H. Zhang, X. Chen, Y. Liu, et al., "PDMS Film-Based Flexible Pressure Sensor Array with Surface Protruding Structure for Human Motion Detection and Wrist Posture Recognition," *ACS Applied Materials & Interfaces* 16, no. 2 (2024): 2554–2563, <https://doi.org/10.1021/acsami.3c14036>.
43. C. Wang, D. Gong, P. Feng, et al., "Ultra-Sensitive and Wide Sensing-Range Flexible Pressure Sensors Based on the Carbon Nanotube Film/Stress-Induced Square Frustum Structure," *ACS Applied Materials & Interfaces* 15, no. 6 (2023): 8546–8554, <https://doi.org/10.1021/acsami.2c22727>.
44. Y. Jeong, J. Gu, J. Byun, et al., "Ultra-Wide Range Pressure Sensor Based on a Microstructured Conductive Nanocomposite for Wearable Workout Monitoring," *Advanced Healthcare Materials* 10, no. 9 (2021): e2001461, <https://doi.org/10.1002/adhm.202001461>.
45. M. Kumari, R. K. Prasad, M. K. Singh, P. K. Iyer, and D. K. Singh, "Piezoresistive/Piezoelectric Pressure Sensor Based on CVD-Grown ZnO Nanowires on Polyethylene Terephthalate Substrate," *ACS Applied Electronic Materials* 6, no. 8 (2024): 6165–6173, <https://doi.org/10.1021/acsaelm.4c00991>.
46. Y. Yang, Y. Yang, Y. Cao, et al., "Anti-Freezing, Resilient and Tough Hydrogels for Sensitive and Large-Range Strain and Pressure Sensors," *Chemical Engineering Journal* 403 (2021): 126431, <https://doi.org/10.1016/j.cej.2020.126431>.
47. X. Cui, J. Chen, W. Wu, et al., "Flexible and Breathable All-Nanofiber Iontronic Pressure Sensors with Ultraviolet Shielding and Antibacterial Performances for Wearable Electronics," *Nano Energy* 95 (2022): 107022, <https://doi.org/10.1016/j.nanoen.2022.107022>.
48. H. Xu, J. Tao, Y. Liu, Y. Mo, R. Bao, and C. Pan, "Fully Fibrous Large-Area Tailorable Triboelectric Nanogenerator Based on Solution Blow Spinning Technology for Energy Harvesting and Self-Powered Sensing," *Small* 18, no. 37 (2022): e2202477, <https://doi.org/10.1002/smll.202202477>.
49. J. Li, X. Pan, Y. Zhang, et al., "Ultrathin Breathable and Stretchable Electronics Based on Patterned Nanofiber Composite Network," *Materials Today Nano* 23 (2023): 100359, <https://doi.org/10.1016/j.mtnano.2023.100359>.
50. Y. Chen, S. Wang, Y. Liu, et al., "Ultra-Low Cost and High-Performance Paper-Based Flexible Pressure Sensor for Artificial Intelligent E-Skin," *Chemical Engineering Journal* 499 (2024): 156293, <https://doi.org/10.1016/j.cej.2024.156293>.
51. T. Zhang, Y. Zhao, Q. Long, et al., "Graphene/MXene/Cellulose Cellulosic Paper-Based Flexible Bifunctional Sensors Utilizing Molecular Bridge Strategy with Tunable Piezoresistive Effect for Temperature-Pressure Sensing," *Chemical Engineering Journal* 497 (2024): 154972, <https://doi.org/10.1016/j.cej.2024.154972>.
52. Y. Li, W. Cao, Z. Liu, Y. Zhang, Z. Chen, and X. Zheng, "A Personalized Electronic Textile for Ultrasensitive Pressure Sensing Enabled by Biocompatible MXene/PEDOT:PSS Composite," *Carbon Energy* 6, no. 3 (2024): e530, <https://doi.org/10.1002/cey2.530>.
53. D. Gan, Z. Huang, X. Wang, et al., "Graphene Oxide-Templated Conductive and Redox-Active Nanosheets Incorporated Hydrogels for Adhesive Bioelectronics," *Advanced Functional Materials* 30, no. 5 (2019): 1907678, <https://doi.org/10.1002/adfm.201907678>.
54. C. B. Cooper, S. E. Root, L. Michalek, et al., "Autonomous Alignment and Healing in Multilayer Soft Electronics Using Immiscible Dynamic Polymers," *Science* 380, no. 6648 (2023): 935–941, <https://doi.org/10.1126/science.adh0619>.
55. M. Morais, E. Carlos, A. Rovisco, et al., "Flexographic Printed Microwave-Assisted Grown Zinc Oxide Nanostructures for Sensing Applications," *Materials Horizons* 11, no. 24 (2024): 6463–6475, <https://doi.org/10.1039/d4mh01000k>.
56. Z. X. Huang, L. W. Li, Y. Z. Huang, et al., "Self-Poled Piezoelectric Polymer Composites via Melt-State Energy Implantation," *Nature Communications* 15, no. 1 (2024): 819, <https://doi.org/10.1038/s41467-024-45184-4>.
57. X. Li, G. Wu, C. Pan, and R. Bao, "Recent Progress in Flexible Sensors Based on 2D Materials," *Journal of Semiconductors* 46, no. 1 (2025): 011607, <https://doi.org/10.1088/1674-4926/24090044>.
58. Y. Mo, X. Feng, L. Zhang, R. Han, R. Bao, and C. Pan, "Tuning the Light Emission of a Si Micropillar Quantum Dot Light-Emitting Device Array with the Strain Coupling Effect," *NPG Asia Materials* 14, no. 1 (2022): 83, <https://doi.org/10.1038/s41427-022-00430-3>.
59. T. Xu, Q. Song, K. Liu, et al., "Nanocellulose-Assisted Construction of Multifunctional MXene-Based Aerogels with Engineering Biomimetic Texture for Pressure Sensor and Compressible Electrode," *Nano-Micro Letters* 15, no. 1 (2023): 98, <https://doi.org/10.1007/s40820-023-01073-x>.
60. T. Yasuda, R. Komine, R. Nijiri, et al., "Ultra-Rapidly Responsive Electret-Based Flexible Pressure Sensor via Functional Polymeric Nanoparticle Synthesis," *Advanced Functional Materials* 34, no. 51 (2024): 2402064, <https://doi.org/10.1002/adfm.202402064>.
61. G. Yang, X. Zheng, J. Li, et al., "Schottky Effect-Enabled High Unit-Area Capacitive Interface for Flexible Pressure Sensors," *Advanced Functional Materials* 34, no. 28 (2024): 2401415, <https://doi.org/10.1002/adfm.202401415>.
62. K. Chen, H. Yang, A. Wang, et al., "Smart Driving Hardware Augmentation by Flexible Piezoresistive Sensor Matrices with Grafted-on Anticreep Composites," *Advanced Science* 12, no. 3 (2025): e2408313, <https://doi.org/10.1002/advs.202408313>.
63. X. He, B. Zhang, Q. Liu, et al., "Highly Conductive and Stretchable Nanostructured Ionogels for 3D Printing Capacitive Sensors with Superior Performance," *Nature Communications* 15, no. 1 (2024): 6431, <https://doi.org/10.1038/s41467-024-50797-w>.
64. X. Pan, Z. Xu, R. Bao, and C. Pan, "Research Progress in Stretchable Circuits: Materials, Methods, and Applications," *Advanced Sensor Research* 2, no. 11 (2023): 2300065, <https://doi.org/10.1002/asdr.202300065>.
65. B. Lee, H. Cho, S. Moon, et al., "Omnidirectional Printing of Elastic Conductors for Three-Dimensional Stretchable Electronics," *Nature Electronics* 6, no. 4 (2023): 307–318, <https://doi.org/10.1038/s41928-023-00949-5>.
66. J. Cao, X. Liu, J. Qiu, et al., "Anti-Friction Gold-Based Stretchable Electronics Enabled by Interfacial Diffusion-Induced Cohesion," *Nature Communications* 15, no. 1 (2024): 1116, <https://doi.org/10.1038/s41467-024-45393-x>.
67. Y. Jiang, S. Ji, J. Sun, et al., "A Universal Interface for Plug-and-Play Assembly of Stretchable Devices," *Nature* 614, no. 7948 (2023): 456–462, <https://doi.org/10.1038/s41586-022-05579-z>.
68. X. Li, Y. Lin, L. Cui, et al., "Stretchable and Lithography-Compatible Interconnects Enabled by Self-Assembled Nanofilms with Interlocking



- Interfaces,” *ACS Applied Materials & Interfaces* 15, no. 48 (2023): 56233–56241, <https://doi.org/10.1021/acsami.3c11760>.
69. X. Li, G. Wu, C. Gao, R. Bao, and C. Pan, “Flexible Electronic Devices and Wearable Sensors Based on Liquid Metals,” *MetalMat* 2, no. 1 (2025): e70000, <https://doi.org/10.1002/metm.70000>.
70. Q. Xiang, G. Zhao, T. Tang, et al., “All-Carbon Piezoresistive Sensor: Enhanced Sensitivity and Wide Linear Range via Multiscale Design for Wearable Applications,” *Advanced Functional Materials* 35, no. 15 (2024): 2418706, <https://doi.org/10.1002/adfm.202418706>.
71. W. Liu, Z. Du, Z. Duan, L. Li, and G. Shen, “Neuroprosthetic Contact Lens Enabled Sensorimotor System for Point-of-Care Monitoring and Feedback of Intraocular Pressure,” *Nature Communications* 15, no. 1 (2024): 5635, <https://doi.org/10.1038/s41467-024-49907-5>.
72. R. Blau, A. Abdal, N. Root, et al., “Conductive Block Copolymer Elastomers and Psychophysical Thresholding for Accurate Haptic Effects,” *Science Robotics* 9, no. 91 (2024): eadk3925, <https://doi.org/10.1126/scirobotics.adk3925>.
73. S. Yang, J. Cheng, J. Shang, et al., “Stretchable Surface Electromyography Electrode Array Patch for Tendon Location and Muscle Injury Prevention,” *Nature Communications* 14, no. 1 (2023): 6494, <https://doi.org/10.1038/s41467-023-42149-x>.
74. S. Zheng, X. Wang, W. Li, Z. Liu, Q. Li, and F. Yan, “Pressure-Stamped Stretchable Electronics Using a Nanofibre Membrane Containing Semi-Embedded Liquid Metal Particles,” *Nature Electronics* 7, no. 7 (2024): 576–585, <https://doi.org/10.1038/s41928-024-01194-0>.
75. X. Chen, B. Wang, J. Duan, et al., “Compression-Durable Soft Electronic Circuits Enabled by Embedding Self-Healing Biphasic Liquid-Solid Metal Into Microstructured Elastomeric Channels,” *Advanced Materials* 37, no. 21 (2025): e2420469, <https://doi.org/10.1002/adma.202420469>.
76. Y. S. Kim, M. Mahmood, Y. Lee, et al., “All-in-One, Wireless, Stretchable Hybrid Electronics for Smart, Connected, and Ambulatory Physiological Monitoring,” *Advanced Science* 6, no. 17 (2019): 1900939, <https://doi.org/10.1002/advs.201900939>.
77. H. Song, G. Luo, Z. Ji, et al., “Highly-Integrated, Miniaturized, Stretchable Electronic Systems Based on Stacked Multilayer Network Materials,” *Science Advances* 8, no. 11 (2022): eabm3785, <https://doi.org/10.1126/sciadv.abm3785>.
78. L. Shi, Z. Li, M. Chen, Y. Qin, Y. Jiang, and L. Wu, “Quantum Effect-Based Flexible and Transparent Pressure Sensors with Ultrahigh Sensitivity and Sensing Density,” *Nature Communications* 11, no. 1 (2020): 3529, <https://doi.org/10.1038/s41467-020-17298-y>.
79. Q. Shen, M. Jiang, R. Wang, et al., “Liquid Metal-Based Soft, Hermetic, and Wireless-Communicable Seals for Stretchable Systems,” *Science* 379, no. 6631 (2023): 488–493, <https://doi.org/10.1126/science.adf7341>.
80. H. Xu, L. Gao, Y. Wang, et al., “Flexible Waterproof Piezoresistive Pressure Sensors with Wide Linear Working Range Based on Conductive Fabrics,” *Nano-Micro Letters* 12, no. 1 (2020): 159, <https://doi.org/10.1007/s40820-020-00498-y>.
81. H. Yuan, T. Zhu, Y. Huang, et al., “Hydrophobic and Adhesive Elastomer Encapsulation for Anti-Drying, Non-Swelling, and Adhesive Hydrogels,” *Advanced Functional Materials* 34, no. 51 (2024): 2409703, <https://doi.org/10.1002/adfm.202409703>.
82. Y. Shao, J. Yan, Y. Zhi, et al., “A Universal Packaging Substrate for Mechanically Stable Assembly of Stretchable Electronics,” *Nature Communications* 15, no. 1 (2024): 6106, <https://doi.org/10.1038/s41467-024-50494-8>.
83. Q. Zhuang, K. Yao, C. Zhang, et al., “Permeable, Three-Dimensional Integrated Electronic Skins with Stretchable Hybrid Liquid Metal Solders,” *Nature Electronics* 7, no. 7 (2024): 598–609, <https://doi.org/10.1038/s41928-024-01189-x>.
84. W. Yan, G. Noel, G. Loke, et al., “Single Fibre Enables Acoustic Fabrics via Nanometre-Scale Vibrations,” *Nature* 603, no. 7902 (2022): 616–623, <https://doi.org/10.1038/s41586-022-04476-9>.
85. J. Hu, Y. Liu, C. Yang, et al., “The Evolution of Underwater Microelectronic Encapsulation: An Universal Marine Wearable Hydrogel,” *Advanced Functional Materials* 35, no. 14 (2024): 2418681, <https://doi.org/10.1002/adfm.202418681>.
86. B. Zhang, J. Li, J. Zhou, et al., “A Three-Dimensional Liquid Diode for Soft, Integrated Permeable Electronics,” *Nature* 628, no. 8006 (2024): 84–92, <https://doi.org/10.1038/s41586-024-07161-1>.
87. P. Sun, Z. Fang, W. Sima, et al., “Microstructured Self-Healing Flexible Tactile Sensors Inspired by Bamboo Leaves,” *ACS Applied Materials & Interfaces* 16, no. 44 (2024): 60699–60714, <https://doi.org/10.1021/acsami.4c15197>.
88. Y. Cheng, Y. Xie, H. Cao, et al., “High-Strength MXene Sheets through Interlayer Hydrogen Bonding for Self-Healing Flexible Pressure Sensor,” *Chemical Engineering Journal* 453 (2023): 139823, <https://doi.org/10.1016/j.cej.2022.139823>.
89. Z. Shen, C. Yang, C. Yao, et al., “Capacitive-Piezoresistive Hybrid Flexible Pressure Sensor Based on Conductive Micropillar Arrays with High Sensitivity over a Wide Dynamic Range,” *Materials Horizons* 10, no. 2 (2023): 499–511, <https://doi.org/10.1039/d2mh00892k>.
90. M. Jiang, H. Hu, C. Jin, et al., “Three-Directional Spacer-Knitted Piezoresistant Strain and Pressure Sensor for Electronic Integration and On-Body Applications,” *ACS Applied Materials & Interfaces* 15, no. 47 (2023): 55009–55021, <https://doi.org/10.1021/acsami.3c09238>.
91. Z. Li, K. Zhao, J. Wang, et al., “Sensitive, Robust, Wide-Range, and High-Consistency Capacitive Tactile Sensors with Ordered Porous Dielectric Microstructures,” *ACS Applied Materials & Interfaces* 16, no. 6 (2024): 7384–7398, <https://doi.org/10.1021/acsami.3c15368>.
92. L. Zhen, M. Cui, X. Bai, et al., “Thin, Flexible Hybrid-Structured Piezoelectric Sensor Array with Enhanced Resolution and Sensitivity,” *Nano Energy* 131 (2024): 110188, <https://doi.org/10.1016/j.nanoen.2024.110188>.
93. S. Qin, P. Yang, Z. Liu, et al., “Triboelectric Sensor with Ultra-Wide Linear Range Based on Water-Containing Elastomer and Ion-Rich Interface,” *Nature Communications* 15, no. 1 (2024): 10640, <https://doi.org/10.1038/s41467-024-54980-x>.
94. B. Zheng, R. Guo, X. Dou, et al., “Blade-Coated Porous 3D Carbon Composite Electrodes Coupled with Multiscale Interfaces for Highly Sensitive All-Paper Pressure Sensors,” *Nano-Micro Letters* 16, no. 1 (2024): 267, <https://doi.org/10.1007/s40820-024-01488-0>.
95. Y. M. Yuan, B. Liu, M. R. Adibeig, et al., “Microstructured Polyelectrolyte Elastomer-Based Ionotronic Sensors with High Sensitivities and Excellent Stability for Artificial Skins,” *Advanced Materials* 36, no. 11 (2024): e2310429, <https://doi.org/10.1002/adma.202310429>.
96. G. Sun, P. Wang, and C. Meng, “Flexible and Breathable Ionotronic Tactile Sensor with Personal Thermal Management Ability for a Comfortable Skin-Attached Sensing Application,” *Nano Energy* 118 (2023): 109006, <https://doi.org/10.1016/j.nanoen.2023.109006>.
97. Y. Wu, S. Dong, X. Li, et al., “A Stretchable All-Nanofiber Ionotronic Pressure Sensor,” *Soft Science* 3, no. 4 (2023): 33, <https://doi.org/10.20517/ss.2023.24>.
98. K. Wang, Y. Yao, H. Liu, et al., “Fabrication of Flexible Wearable Mechanosensors Utilizing Piezoelectric Hydrogels Mechanically Enhanced by Dipole-Dipole Interactions,” *ACS Applied Materials & Interfaces* 16, no. 38 (2024): 51542–51553, <https://doi.org/10.1021/acsami.4c11569>.
99. Q. Zhang, J. Li, G. Li, et al., “Hierarchically Structured Hollow PVDF Nanofibers for Flexible Piezoelectric Sensor,” *Chemical Engineering Journal* 498 (2024): 155661, <https://doi.org/10.1016/j.cej.2024.155661>.

100. X. He, Z. Cui, F. Zhang, et al., "Multiscale Heterogeneities-Based Piezoresistive Interfaces with Ultralow Detection Limitation and Adaptively Switchable Pressure Detectability," *ACS Nano* 18, no. 11 (2024): 8296–8306, <https://doi.org/10.1021/acsnano.3c12513>.
101. X. Qu, J. Li, Z. Han, et al., "Highly Sensitive Fiber Pressure Sensors over a Wide Pressure Range Enabled by Resistive-Capacitive Hybrid Response," *ACS Nano* 17, no. 15 (2023): 14904–14915, <https://doi.org/10.1021/acsnano.3c03484>.
102. C. Lv, C. Tian, J. Jiang, et al., "Ultrasensitive Linear Capacitive Pressure Sensor with Wrinkled Microstructures for Tactile Perception," *Advanced Science* 10, no. 14 (2023): e2206807, <https://doi.org/10.1002/advs.202206807>.
103. W. Hong, X. Guo, T. Zhang, et al., "Flexible Capacitive Pressure Sensor with High Sensitivity and Wide Range Based on a Cheetah Leg Structure via 3D Printing," *ACS Applied Materials & Interfaces* 15, no. 39 (2023): 46347–46356, <https://doi.org/10.1021/acsami.3c09841>.
104. G. Wu, X. Li, R. Bao, and C. Pan, "Innovations in Tactile Sensing: Microstructural Designs for Superior Flexible Sensor Performance," *Advanced Functional Materials* 34, no. 44 (2024): 2405722, <https://doi.org/10.1002/adfm.202405722>.
105. Y. Liu, J. Tao, Y. Mo, R. Bao, and C. Pan, "Ultrasensitive Touch Sensor for Simultaneous Tactile and Slip Sensing," *Advanced Materials* 36, no. 21 (2024): e2313857, <https://doi.org/10.1002/adma.202313857>.
106. G. Li, Y. Zhang, X. Zhang, et al., "Filiform Papillae-Inspired Wearable Pressure Sensor with High Sensitivity and Wide Detection Range," *Advanced Functional Materials* 35, no. 5 (2024): 2414465, <https://doi.org/10.1002/adfm.202414465>.
107. R. Chen, T. Luo, J. Wang, et al., "Nonlinearity Synergy: An Elegant Strategy for Realizing High-Sensitivity and Wide-Linear-Range Pressure Sensing," *Nature Communications* 14, no. 1 (2023): 6641, <https://doi.org/10.1038/s41467-023-42361-9>.
108. J. Chen, K. Chen, J. Jin, et al., "Outstanding Synergy of Sensitivity and Linear Range Enabled by Multigradient Architectures," *Nano Letters* 23, no. 24 (2023): 11958–11967, <https://doi.org/10.1021/acs.nanolett.3c04204>.
109. J. Zhao, H. Guo, H. Liu, et al., "Carbon Nanotube Network Topology-Enhanced Iontronic Capacitive Pressure Sensor with High Linearity and Ultrahigh Sensitivity," *ACS Applied Materials & Interfaces* 15, no. 40 (2023): 47327–47337, <https://doi.org/10.1021/acsami.3c10100>.
110. J. He, S. Wang, R. Han, et al., "Wide Detection Range Flexible Pressure Sensors Based on 3D Interlocking Structure TPU/ZnO NWs," *Advanced Functional Materials* 35, no. 15 (2024): 2418791, <https://doi.org/10.1002/adfm.202418791>.
111. J. Yang, Z. Li, Y. Wu, et al., "Non-Equilibrium Compression Achieving High Sensitivity and Linearity for Iontronic Pressure Sensors," *Science Bulletin* 69, no. 14 (2024): 2221–2230, <https://doi.org/10.1016/j.scib.2024.05.001>.
112. X. H. Zhao, Q. T. Lai, W. T. Guo, et al., "Skin-Inspired Highly Sensitive Tactile Sensors with Ultrahigh Resolution over a Broad Sensing Range," *ACS Applied Materials & Interfaces* 15, no. 25 (2023): 30486–30494, <https://doi.org/10.1021/acsami.3c04526>.
113. C. Gui, D. Wang, J. Cao, and S. Feng, "Efficient Fabrication of Conductive Sponges for Wearable Flexible Sensors," *Chemical Engineering Journal* 499 (2024): 156251, <https://doi.org/10.1016/j.cej.2024.156251>.
114. R. Yang, A. Dutta, B. Li, et al., "Iontronic Pressure Sensor with High Sensitivity over Ultra-Broad Linear Range Enabled by Laser-Induced Gradient Micro-Pyramids," *Nature Communications* 14, no. 1 (2023): 2907, <https://doi.org/10.1038/s41467-023-38274-2>.
115. J. Baek, Y. Zhang, F. Qin, et al., "Design Rules for 3D Printing-Assisted Pressure Sensor Manufacturing: Achieving Broad Pressure Range Linearity," *Advanced Functional Materials* 35, no. 4 (2024): 2414050, <https://doi.org/10.1002/adfm.202414050>.
116. N. Li, S. Gao, Y. Li, J. Liu, W. Song, and G. Shen, "Multi-Attribute Wearable Pressure Sensor Based on Multilayered Modulation with High Constant Sensitivity over a Wide Range," *Nano Research* 16, no. 5 (2023): 7583–7592, <https://doi.org/10.1007/s12274-022-5371-6>.
117. S. Wu, C. Yang, J. Hu, et al., "Normal-Direction Graded Hemispheres for Ionic Flexible Sensors with a Record-High Linearity in a Wide Working Range," *ACS Applied Materials & Interfaces* 15, no. 40 (2023): 47733–47744, <https://doi.org/10.1021/acsami.3c09580>.
118. Z. Han, L. Mo, S. Han, et al., "Flexible Sensors with Enhanced Sensitivity and Broadened Detection Range Through Conformal Printing and Space-Confined Design," *Small* 21, no. 5 (2025): e2407168, <https://doi.org/10.1002/sml.202407168>.
119. Y. Zhang, J. Yang, X. Hou, et al., "Highly Stable Flexible Pressure Sensors with a Quasi-Homogeneous Composition and Interlinked Interfaces," *Nature Communications* 13, no. 1 (2022): 1317, <https://doi.org/10.1038/s41467-022-29093-y>.
120. Y. He, Y. Cheng, C. Yang, and C. F. Guo, "Creep-Free Polyelectrolyte Elastomer for Drift-Free Iontronic Sensing," *Nature Materials* 23, no. 8 (2024): 1107–1114, <https://doi.org/10.1038/s41563-024-01848-6>.
121. Y. Zhang, X. Zhou, N. Zhang, et al., "Ultrafast Piezocapacitive Soft Pressure Sensors with over 10 kHz Bandwidth via Bonded Microstructured Interfaces," *Nature Communications* 15, no. 1 (2024): 3048, <https://doi.org/10.1038/s41467-024-47408-z>.
122. S. B. Choi, T. Noh, S. B. Jung, and J. W. Kim, "Stretchable Piezoresistive Pressure Sensor Array with Sophisticated Sensitivity, Strain-Insensitivity, and Reproducibility," *Advanced Science* 11, no. 35 (2024): e2405374, <https://doi.org/10.1002/advs.202405374>.
123. Y. Zhang, Q. Lu, J. He, et al., "Localizing Strain via Micro-Cage Structure for Stretchable Pressure Sensor Arrays with Ultralow Spatial Crosstalk," *Nature Communications* 14, no. 1 (2023): 1252, <https://doi.org/10.1038/s41467-023-36885-3>.
124. B. Sun, Z. Li, Z. Song, et al., "Gradient Modulus Strategy for Alleviating Stretchable Electronic Strain Concentration," *Advanced Functional Materials* 34, no. 52 (2024): 2410676, <https://doi.org/10.1002/adfm.202410676>.
125. B. Aksoy, Y. Hao, G. Grasso, K. M. Digumarti, V. Cacucciolo, and H. Shea, "Shielded Soft Force Sensors," *Nature Communications* 13, no. 1 (2022): 4649, <https://doi.org/10.1038/s41467-022-32391-0>.
126. B. Zhu, J. Guo, W. Li, et al., "Integrated Electromechanical Structure for Iontronic Pressure Sensors with Linear High-Sensitivity Response and Robust Sensing Stability," *Advanced Functional Materials* 34, no. 42 (2024): 2406762, <https://doi.org/10.1002/adfm.202406762>.
127. R. Han, Y. Liu, Y. Mo, et al., "High Anti-Jamming Flexible Capacitive Pressure Sensors Based on Core-Shell Structured AgNWs@TiO<sub>2</sub>," *Advanced Functional Materials* 33, no. 51 (2023): 2305531, <https://doi.org/10.1002/adfm.202305531>.
128. H.-C. Xu, Y. Liu, Y.-P. Mo, et al., "All-Fiber Anti-Jamming Capacitive Pressure Sensors Based on Liquid Metals," *Rare Metals* 44, no. 7 (2025): 4839–4850, <https://doi.org/10.1007/s12598-024-03071-3>.
129. M. I. Jordan and T. M. Mitchell, "Machine Learning: Trends, Perspectives, and Prospects," *Science* 349, no. 6245 (2015): 255–260, <https://doi.org/10.1126/science.aaa8415>.
130. J. Lee, J. Y. Kwak, K. Keum, et al., "Recent Advances in Smart Tactile Sensory Systems with Brain-Inspired Neural Networks," *Advanced Intelligent Systems* 6, no. 4 (2024): 2300631, <https://doi.org/10.1002/aisy.202300631>.
131. M. Wang, T. Wang, Y. Luo, et al., "Fusing Stretchable Sensing Technology with Machine Learning for Human–Machine Interfaces," *Advanced Functional Materials* 31, no. 39 (2021): 2008807, <https://doi.org/10.1002/adfm.202008807>.

132. M. Mahmood, D. Mzurikwao, Y.-S. Kim, et al., "Fully Portable and Wireless Universal Brain-machine Interfaces Enabled by Flexible Scalp Electronics and Deep Learning Algorithm," *Nature Machine Intelligence* 1, no. 9 (2019): 412–422, <https://doi.org/10.1038/s42256-019-0091-7>.
133. V. A. Ho, M. Makikawa, and S. Hirai, "Flexible Fabric Sensor Toward a Humanoid Robot's Skin: Fabrication, Characterization, and Perceptions," *IEEE Sensors Journal* 13, no. 10 (2013): 4065–4080, <https://doi.org/10.1109/jsen.2013.2272336>.
134. Q. Shi, Z. Zhang, T. He, et al., "Deep Learning Enabled Smart Mats as a Scalable Floor Monitoring System," *Nature Communications* 11, no. 1 (2020): 4609, <https://doi.org/10.1038/s41467-020-18471-z>.
135. M. Alameh, Y. Abbass, A. Ibrahim, G. Moser, and M. Valle, "Touch Modality Classification Using Recurrent Neural Networks," *IEEE Sensors Journal* 21, no. 8 (2021): 9983–9993, <https://doi.org/10.1109/jsen.2021.3055565>.
136. N. Dai, I. M. Lei, Z. Li, Y. Li, P. Fang, and J. Zhong, "Recent Advances in Wearable Electromechanical Sensors—Moving towards Machine Learning-Assisted Wearable Sensing Systems," *Nano Energy* 105 (2023): 108041, <https://doi.org/10.1016/j.nanoen.2022.108041>.
137. M. Khorsand, J. Tavakoli, H. Guan, and Y. Tang, "Artificial Intelligence Enhanced Mathematical Modeling on Rotary Triboelectric Nanogenerators under Various Kinematic and Geometric Conditions," *Nano Energy* 75 (2020): 104993, <https://doi.org/10.1016/j.nanoen.2020.104993>.
138. Y. Tang, G. Li, T. Zhang, et al., "Digital Channel-Enabled Distributed Force Decoding via Small Datasets for Hand-Centric Interactions," *Science Advances* 11, no. 4 (2025): eadt2641, <https://doi.org/10.1126/sciadv.adt2641>.
139. K. Kim, J. H. Hong, K. Bae, et al., "Extremely Durable Electrical Impedance Tomography-Based Soft and Ultrathin Wearable E-Skin for Three-Dimensional Tactile Interfaces," *Science Advances* 10, no. 38 (2024): eadr1099, <https://doi.org/10.1126/sciadv.adr1099>.
140. Y. Luo, C. Liu, Y. J. Lee, et al., "Adaptive Tactile Interaction Transfer via Digitally Embroidered Smart Gloves," *Nature Communications* 15, no. 1 (2024): 868, <https://doi.org/10.1038/s41467-024-45059-8>.
141. D. Kong, Y. Lu, S. Zhou, et al., "Super-Resolution Tactile Sensor Arrays with Sparse Units Enabled by Deep Learning," *Science Advances* 11, no. 27 (2025): eadv2124, <https://doi.org/10.1126/sciadv.adv2124>.
142. M. Iskandar, A. Albu-Schaffer, and A. Dietrich, "Intrinsic Sense of Touch for Intuitive Physical Human-Robot Interaction," *Science Robotics* 9, no. 93 (2024): eadn4008, <https://doi.org/10.1126/scirobotics.adn4008>.
143. N. T. Beigh, F. T. Beigh, and D. Mallick, "Machine Learning Assisted Hybrid Transduction Nanocomposite Based Flexible Pressure Sensor Matrix for Human Gait Analysis," *Nano Energy* 116 (2023): 108824, <https://doi.org/10.1016/j.nanoen.2023.108824>.
144. N. Bai, Y. Xue, S. Chen, et al., "A Robotic Sensory System with High Spatiotemporal Resolution for Texture Recognition," *Nature Communications* 14, no. 1 (2023): 7121, <https://doi.org/10.1038/s41467-023-42722-4>.
145. S. Potluri, A. B. Chandran, C. Diedrich, and L. Schega, "Machine Learning Based Human Gait Segmentation with Wearable Sensor Platform," *Annual International Conference of the IEEE Engineering in Medicine and Biology Society* 2019 (2019): 588–594, <https://doi.org/10.1109/EMBC.2019.8857509>.
146. W. Lin, Z. Wang, Y. Xu, et al., "Self-Adaptive Perception of Object's Deformability with Multiple Deformation Attributes Utilizing Biomimetic Mechanoreceptors," *Advanced Materials* 36, no. 9 (2024): e2305032, <https://doi.org/10.1002/adma.202305032>.
147. S. Wang, X. Fan, Z. Zhang, et al., "A Skin-Inspired High-Performance Tactile Sensor for Accurate Recognition of Object Softness," *ACS Nano* 18, no. 26 (2024): 17175–17184, <https://doi.org/10.1021/acsnano.4c04100>.
148. S. Lee, J. Jang, and W. Park, "A Tactile Sensor for Recognition of Softness Using Interlocking Structure of Carbon Nanoparticle-Polydimethylsiloxane Composite," *Sensors and Actuators Reports* 9 (2025): 100289, <https://doi.org/10.1016/j.snr.2025.100289>.
149. H. Qiao, S. Sun, and P. Wu, "Non-Equilibrium-Growing Aesthetic Ionic Skin for Fingertip-Like Strain-Undisturbed Tactile Sensation and Texture Recognition," *Advanced Materials* 35, no. 21 (2023): e2300593, <https://doi.org/10.1002/adma.202300593>.
150. X. Guo, Z. Sun, Y. Zhu, and C. Lee, "Zero-Biased Bionic Fingertip E-Skin with Multimodal Tactile Perception and Artificial Intelligence for Augmented Touch Awareness," *Advanced Materials* 36, no. 39 (2024): e2406778, <https://doi.org/10.1002/adma.202406778>.
151. Y. Wang, J. Zhao, X. Zeng, et al., "All-Printed Finger-Inspired Tactile Sensor Array for Microscale Texture Detection and 3D Reconstruction," *Advanced Science* 11, no. 26 (2024): e2400479, <https://doi.org/10.1002/advs.202400479>.
152. S. Sundaram, P. Kellnhofer, Y. Li, J. Y. Zhu, A. Torralba, and W. Matusik, "Learning the Signatures of the Human Grasp Using a Scalable Tactile Glove," *Nature* 569, no. 7758 (2019): 698–702, <https://doi.org/10.1038/s41586-019-1234-z>.
153. G. Chen, Y. Zhang, S. Li, et al., "Flexible Artificial Tactility with Excellent Robustness and Temperature Tolerance Based on Organohydrogel Sensor Array for Robot Motion Detection and Object Shape Recognition," *Advanced Materials* 36, no. 45 (2024): e2408193, <https://doi.org/10.1002/adma.202408193>.
154. Y. Qiu, F. Wang, Z. Zhang, et al., "Quantitative Softness and Texture Bimodal Haptic Sensors for Robotic Clinical Feature Identification and Intelligent Picking," *Science Advances* 10, no. 30 (2024): eadp0348, <https://doi.org/10.1126/sciadv.adp0348>.
155. S. J. Hong, Y. R. Lee, A. Bag, et al., "Bio-Inspired Artificial Mechanoreceptors with Built-in Synaptic Functions for Intelligent Tactile Skin," *Nature Materials* 24, no. 7 (2025): 1100–1108, <https://doi.org/10.1038/s41563-025-02204-y>.
156. S. Tian, L. Wang, and R. Zhu, "A Flexible Multimodal Pulse Sensor for Wearable Continuous Blood Pressure Monitoring," *Materials Horizons* 11, no. 10 (2024): 2428–2437, <https://doi.org/10.1039/d3mh01999c>.
157. Q. Mao, Z. Liao, J. Yuan, and R. Zhu, "Multimodal Tactile Sensing Fused with Vision for Dexterous Robotic Housekeeping," *Nature Communications* 15, no. 1 (2024): 6871, <https://doi.org/10.1038/s41467-024-51261-5>.
158. C. Han, Z. Cao, Z. An, Z. Zhang, Z. L. Wang, and Z. Wu, "Multimodal Finger-Shaped Tactile Sensor for Multi-Directional Force and Material Identification," *Advanced Materials* 37, no. 19 (2025): e2414096, <https://doi.org/10.1002/adma.202414096>.
159. S. Chen, G. Qian, B. Ghanem, et al., "Quantitative and Real-Time Evaluation of Human Respiration Signals with a Shape-Conformal Wireless Sensing System," *Advanced Science* 9, no. 32 (2022): e2203460, <https://doi.org/10.1002/advs.202203460>.
160. Z. Sun, M. Zhu, Z. Zhang, et al., "Artificial Intelligence of Things (AIoT) Enabled Virtual Shop Applications Using Self-Powered Sensor Enhanced Soft Robotic Manipulator," *Advanced Science* 8, no. 14 (2021): e2100230, <https://doi.org/10.1002/advs.202100230>.
161. B. Li, L. Li, H. Wang, G. Chen, B. Wang, and S. Qiu, "TVT-Transformer: A Tactile-Visual-Textual Fusion Network for Object Recognition," *Information Fusion* 118 (2025): 102943, <https://doi.org/10.1016/j.inffus.2025.102943>.
162. W.-Q. Wu, C.-F. Wang, S.-T. Han, and C.-F. Pan, "Recent Advances in Imaging Devices: Image Sensors and Neuromorphic Vision Sensors," *Rare Metals* 43, no. 11 (2024): 5487–5515, <https://doi.org/10.1007/s12598-024-02811-9>.



163. S. Suresh, H. Qi, T. Wu, et al., "NeuralFeels with Neural Fields: Visuotactile Perception for in-Hand Manipulation," *Science Robotics* 9, no. 96 (2024): eadl0628, <https://doi.org/10.1126/scirobotics.adl0628>.
164. C. Jiang, W. Xu, Y. Li, et al., "Capturing Forceful Interaction with Deformable Objects Using a Deep Learning-Powered Stretchable Tactile Array," *Nature Communications* 15, no. 1 (2024): 9513, <https://doi.org/10.1038/s41467-024-53654-y>.
165. X. Liang, H. Li, W. Wang, et al., "Fusion of Wearable and Contactless Sensors for Intelligent Gesture Recognition," *Advanced Intelligent Systems* 1, no. 7 (2019): 1900088, <https://doi.org/10.1002/aisy.201900088>.
166. J. H. Lee, J. S. Heo, Y. J. Kim, et al., "A Behavior-Learned Cross-Reactive Sensor Matrix for Intelligent Skin Perception," *Advanced Materials* 32, no. 22 (2020): e2000969, <https://doi.org/10.1002/adma.202000969>.
167. J. Gu, H. Wang, D. Li, X. Zhang, X. Ji, and J. Liang, "Artificial Flexible Closed-Loop Tactile Systems," *Advanced Materials Technologies* 10, no. 12 (2025): 2402052, <https://doi.org/10.1002/admt.202402052>.
168. J. Yin, R. Hinchet, H. Shea, and C. Majidi, "Wearable Soft Technologies for Haptic Sensing and Feedback," *Advanced Functional Materials* 31, no. 39 (2020): 2007428, <https://doi.org/10.1002/adfm.202007428>.
169. S. B. Moqadam, K. Delle, U. Schorling, A. S. Asheghabadi, F. Norouzi, and J. Xu, "Reproducing Tactile and Proprioception Based on the Human-in-the-Closed-Loop Conceptual Approach," *IEEE Access* 11 (2023): 41894–41905, <https://doi.org/10.1109/access.2023.3267963>.
170. R. Liu, F. Nageotte, P. Zanne, M. de Mathelin, and B. Dresp-Langley, "Deep Reinforcement Learning for the Control of Robotic Manipulation: A Focussed Mini-Review," *Robotics* 10, no. 1 (2021): 22, <https://doi.org/10.3390/robotics10010022>.
171. D. Han, B. Mulyana, V. Stankovic, and S. Cheng, "A Survey on Deep Reinforcement Learning Algorithms for Robotic Manipulation," *Sensors* 23, no. 7 (2023): 3762, <https://doi.org/10.3390/s23073762>.
172. Y. Huang, K. Yao, J. Li, et al., "Recent Advances in Multi-Mode Haptic Feedback Technologies towards Wearable Interfaces," *Materials Today Physics* 22 (2022): 100602, <https://doi.org/10.1016/j.mtphys.2021.100602>.
173. E. D'Anna, G. Valle, A. Mazzoni, et al., "A Closed-Loop Hand Prosthesis with Simultaneous Intraneural Tactile and Position Feedback," *Science Robotics* 4, no. 27 (2019): eaau8892, <https://doi.org/10.1126/scirobotics.aau8892>.
174. L. Zollo, G. Di Pino, A. L. Ciano, et al., "Restoring Tactile Sensations via Neural Interfaces for Real-Time Force-and-Slippage Closed-Loop Control of Bionic Hands," *Science Robotics* 4, no. 27 (2019): eaau9924, <https://doi.org/10.1126/scirobotics.aau9924>.
175. X. Yang, W. Chen, Q. Fan, et al., "Electronic Skin for Health Monitoring Systems: Properties, Functions, and Applications," *Advanced Materials* 36, no. 31 (2024): e2402542, <https://doi.org/10.1002/adma.202402542>.
176. Q. T. Lai, X. H. Zhao, Q. J. Sun, Z. Tang, X. G. Tang, and V. A. L. Roy, "Emerging MXene-Based Flexible Tactile Sensors for Health Monitoring and Haptic Perception," *Small* 19, no. 27 (2023): e2300283, <https://doi.org/10.1002/sml.202300283>.
177. J. Zhong, Z. Li, M. Takakuwa, et al., "Smart Face Mask Based on an Ultrathin Pressure Sensor for Wireless Monitoring of Breath Conditions," *Advanced Materials* 34, no. 6 (2022): e2107758, <https://doi.org/10.1002/adma.202107758>.
178. M. Zeng, J. Ding, Y. Tian, et al., "Phase Separation Manipulated Gradient Conductivity for A High-Precision Flexible Pressure Sensor," *Advanced Functional Materials* 34, no. 52 (2024): 2411390, <https://doi.org/10.1002/adfm.202411390>.
179. M. Cao, M. Leng, W. Pan, et al., "3D Wearable Piezoresistive Sensor with Waterproof and Antibacterial Activity for Multimodal Smart Sensing," *Nano Energy* 112 (2023): 108492, <https://doi.org/10.1016/j.nanoen.2023.108492>.
180. G. Chen, X. Zhao, S. Andalib, et al., "Discovering Giant Magnetoelasticity in Soft Matter for Electronic Textiles," *Matter* 4, no. 11 (2021): 3725–3740, <https://doi.org/10.1016/j.matt.2021.09.012>.
181. Y. Zhao, Q. Sun, S. Mei, et al., "Wearable Multichannel-Active Pressurized Pulse Sensing Platform," *Microsystems & Nanoengineering* 10 (2024): 77, <https://doi.org/10.1038/s41378-024-00703-7>.
182. W. Xiao, X. Cai, A. Jadoon, et al., "High-Performance Graphene Flexible Sensors for Pulse Monitoring and Human-Machine Interaction," *ACS Applied Materials & Interfaces* 16, no. 25 (2024): 32445–32455, <https://doi.org/10.1021/acsami.4c06546>.
183. J. Li, K. Ma, B. Qin, et al., "An All-in-One Wearable Device Integrating a Solid-State Zinc-Ion Battery and a Capacitive Pressure Sensor for Intelligent Health Monitoring," *Advanced Functional Materials* 34, no. 39 (2024): 2403788, <https://doi.org/10.1002/adfm.202403788>.
184. X. Cui, Y. Jiang, L. Hu, et al., "Synergistically Microstructured Flexible Pressure Sensors with High Sensitivity and Ultrawide Linear Range for Full-Range Human Physiological Monitoring," *Advanced Materials Technologies* 8, no. 1 (2022): 2200609, <https://doi.org/10.1002/admt.202200609>.
185. C. Lu, Y. Gao, X. Chan, et al., "A Cross-Scale Honeycomb Architecture-Based Flexible Piezoresistive Sensor for Multiscale Pressure Perception and Fine-Grained Identification," *Materials Horizons* 11, no. 2 (2024): 510–518, <https://doi.org/10.1039/d3mh01387a>.
186. C. Zhang, Q. Yang, X. Meng, et al., "Wireless, Smart Hemostasis Device with All-Soft Sensing System for Quantitative and Real-Time Pressure Evaluation," *Advanced Science* 10, no. 33 (2023): e2303418, <https://doi.org/10.1002/advs.202303418>.
187. Y. Park, H. Luan, K. Kwon, et al., "Soft, Full Wheatstone Bridge 3D Pressure Sensors for Cardiovascular Monitoring," *npj Flexible Electronics* 8, no. 1 (2024): 6, <https://doi.org/10.1038/s41528-024-00294-3>.
188. X. Kang, J. Zhang, Z. Shao, et al., "A Wearable and Real-Time Pulse Wave Monitoring System Based on a Flexible Compound Sensor," *Biosensors* 12, no. 2 (2022): 133, <https://doi.org/10.3390/bios12020133>.
189. X. Wang, G. Wu, X. Zhang, et al., "Traditional Chinese Medicine (TCM)-Inspired Fully Printed Soft Pressure Sensor Array with Self-Adaptive Pressurization for Highly Reliable Individualized Long-Term Pulse Diagnostics," *Advanced Materials* 37, no. 1 (2025): e2410312, <https://doi.org/10.1002/adma.202410312>.
190. Y. Fang, Y. Zou, J. Xu, et al., "Ambulatory Cardiovascular Monitoring Via a Machine-Learning-Assisted Textile Triboelectric Sensor," *Advanced Materials* 33, no. 41 (2021): e2104178, <https://doi.org/10.1002/adma.202104178>.
191. S. Wang, M. Dong, J. He, et al., "A Multi-User Wearable Waistband System for Real-Time Health Monitoring of Respiration, ECG, and Body Temperature," *Microelectronic Engineering* 299 (2025): 112346, <https://doi.org/10.1016/j.mee.2025.112346>.
192. D. Ma, Q. Wu, H. Fang, et al., "Skin-Core-Fiber-Based Fabric Integrated with Pressure Sensing and Deep Learning for Posture Recognition," *Nano Energy* 132 (2024): 110376, <https://doi.org/10.1016/j.nanoen.2024.110376>.
193. Z. Feng, Q. He, J. Qiu, et al., "Iontronic Textile-Based Capacitive Pressure Sensor for Unconstrained Respiration and Heartbeat Monitoring," *Advanced Materials Technologies* 8, no. 22 (2023): 2300949, <https://doi.org/10.1002/admt.202300949>.
194. L. Wu, X. Li, J. Choi, et al., "Beetle-Inspired Gradient Slant Structures for Capacitive Pressure Sensor with a Broad Linear Response Range," *Advanced Functional Materials* 34, no. 26 (2024): 2312370, <https://doi.org/10.1002/adfm.202312370>.

195. X. Li, Y. Liu, Y. Ding, et al., "Capacitive Pressure Sensor Combining Dual Dielectric Layers with Integrated Composite Electrode for Wearable Healthcare Monitoring," *ACS Applied Materials & Interfaces* 16, no. 10 (2024): 12974–12985, <https://doi.org/10.1021/acsami.4c01042>.
196. Z. Yang, Q. Wang, H. Yu, et al., "Self-Powered Biomimetic Pressure Sensor Based on Mn-Ag Electrochemical Reaction for Monitoring Rehabilitation Training of Athletes," *Advanced Science* 11, no. 25 (2024): e2401515, <https://doi.org/10.1002/advs.202401515>.
197. Q. Wang, H. Guan, C. Wang, et al., "A Wireless, Self-Powered Smart Insole for Gait Monitoring and Recognition via Nonlinear Synergistic Pressure Sensing," *Science Advances* 11, no. 16 (2025): eadu1598, <https://doi.org/10.1126/sciadv.adu1598>.
198. Z. Wang, X. He, T. Bu, et al., "A Full-Process, Fine-Grained, and Quantitative Rehabilitation Assessment Platform Enabled by On-Skin Sensors and Multi-Task Gait Transformer Model," *Advanced Materials* 36, no. 46 (2024): e2408478, <https://doi.org/10.1002/adma.202408478>.
199. Y. Jiang, J. An, F. Liang, et al., "Knitted Self-Powered Sensing Textiles for Machine Learning-Assisted Sitting Posture Monitoring and Correction," *Nano Research* 15, no. 9 (2022): 8389–8397, <https://doi.org/10.1007/s12274-022-4409-0>.
200. D. Liu, D. Zhang, Z. Sun, et al., "Active-Matrix Sensing Array Assisted with Machine-Learning Approach for Lumbar Degenerative Disease Diagnosis and Postoperative Assessment," *Advanced Functional Materials* 32, no. 21 (2022): 2113008, <https://doi.org/10.1002/adfm.202113008>.
201. P. Zhang, X. Zhang, M. Teng, et al., "Leather-Based Shoe Soles for Real-Time Gait Recognition and Automatic Remote Assistance Using Machine Learning," *ACS Applied Materials & Interfaces* 16, no. 45 (2024): 62803–62816, <https://doi.org/10.1021/acsami.4c16505>.
202. D. Guo, Y. Li, Q. Zhou, et al., "Degradable, Biocompatible, and Flexible Capacitive Pressure Sensor for Intelligent Gait Recognition and Rehabilitation Training," *Nano Energy* 127 (2024): 109750, <https://doi.org/10.1016/j.nanoen.2024.109750>.
203. C. Wang, Y. Hu, Y. Liu, et al., "Tissue-Adhesive Piezoelectric Soft Sensor for In Vivo Blood Pressure Monitoring During Surgical Operation," *Advanced Functional Materials* 33, no. 38 (2023): 2303696, <https://doi.org/10.1002/adfm.202303696>.
204. Z. Zhang, Q. Yan, Z. Liu, et al., "Flexible MXene Composed Triboelectric Nanogenerator via Facile Vacuum-Assistant Filtration Method for Self-Powered Biomechanical Sensing," *Nano Energy* 88 (2021): 106257, <https://doi.org/10.1016/j.nanoen.2021.106257>.
205. F. Yin, H. Niu, E. S. Kim, Y. K. Shin, Y. Li, and N. Y. Kim, "Advanced Polymer Materials-Based Electronic Skins for Tactile and Non-Contact Sensing Applications," *InfoMat* 5, no. 7 (2023): e12424, <https://doi.org/10.1002/inf2.12424>.
206. N. Dai, X. Guan, C. Lu, et al., "A Flexible Self-Powered Noncontact Sensor with an Ultrawide Sensing Range for Human-Machine Interactions in Harsh Environments," *ACS Nano* 17, no. 24 (2023): 24814–24825, <https://doi.org/10.1021/acsnano.3c05507>.
207. W. Zhong, H. Xu, Y. Ke, et al., "Accurate and Efficient Sitting Posture Recognition and Human-Machine Interaction Device Based on Fabric Pressure Sensor Array and Neural Network," *Advanced Materials Technologies* 9, no. 3 (2023): 2301579, <https://doi.org/10.1002/admt.202301579>.
208. W. Wu, T. Jiang, M. Wang, et al., "Bioinspired Monopolar Controlled Ionic Hydrogels for Flexible Non-Contact Human-Machine Interfaces," *Advanced Functional Materials* 34, no. 48 (2024): 2408338, <https://doi.org/10.1002/adfm.202408338>.
209. X. Zhi, S. Ma, Y. Xia, et al., "Hybrid Tactile Sensor Array for Pressure Sensing and Tactile Pattern Recognition," *Nano Energy* 125 (2024): 109532, <https://doi.org/10.1016/j.nanoen.2024.109532>.
210. X. Chen, Y. Luo, Y. Chen, et al., "Biomimetic Contact Behavior Inspired Tactile Sensing Array with Programmable Microdome Pattern by Scalable and Consistent Fabrication," *Advanced Science* 11, no. 43 (2024): e2408082, <https://doi.org/10.1002/advs.202408082>.
211. J. Chen, T. Song, X. Wang, et al., "Ultrasensitive and Wide-Range MXene/PDMS Piezoresistive Sensors Inspired by Rose Petals," *Nano Energy* 131 (2024): 110285, <https://doi.org/10.1016/j.nanoen.2024.110285>.
212. B. Hou, D. Yang, X. Ren, L. Yi, and X. Liu, "A Tactile Oral Pad Based on Carbon Nanotubes for Multimodal Haptic Interaction," *Nature Electronics* 7, no. 9 (2024): 777–787, <https://doi.org/10.1038/s41928-024-01234-9>.
213. W. Guo, Z. Ma, Z. Chen, et al., "Thin and Soft Ti3C2Tx MXene Sponge Structure for Highly Sensitive Pressure Sensor Assisted by Deep Learning," *Chemical Engineering Journal* 485 (2024): 149659, <https://doi.org/10.1016/j.cej.2024.149659>.
214. W. Yang, S. Lin, W. Gong, et al., "Single Body-Coupled Fiber Enables Chipless Textile Electronics," *Science* 384, no. 6691 (2024): 74–81, <https://doi.org/10.1126/science.adk3755>.
215. A. Cheng, X. Li, D. Li, et al., "An Intelligent Hybrid-Fabric Wristband System Enabled by Thermal Encapsulation for Ergonomic Human-Machine Interaction," *Nature Communications* 16, no. 1 (2025): 591, <https://doi.org/10.1038/s41467-024-55649-1>.
216. S. Li, J. Tian, K. Li, et al., "Intelligent Song Recognition via a Hollow-Microstructure-Based, Ultrasensitive Artificial Eardrum," *Advanced Science* 11, no. 42 (2024): e2405501, <https://doi.org/10.1002/advs.202405501>.
217. Q. Yang, W. Jin, Q. Zhang, et al., "Mixed-Modality Speech Recognition and Interaction Using a Wearable Artificial Throat," *Nature Machine Intelligence* 5, no. 2 (2023): 169–180, <https://doi.org/10.1038/s42256-023-00616-6>.
218. G. Y. Gou, X. S. Li, J. M. Jian, et al., "Two-Stage Amplification of an Ultrasensitive MXene-Based Intelligent Artificial Eardrum," *Science Advances* 8, no. 13 (2022): eabn2156, <https://doi.org/10.1126/sciadv.abn2156>.
219. T. Liu, M. Zhang, Z. Li, et al., "Machine Learning-Assisted Wearable Sensing Systems for Speech Recognition and Interaction," *Nature Communications* 16, no. 1 (2025): 2363, <https://doi.org/10.1038/s41467-025-57629-5>.
220. X. Lu, H. Tan, H. Zhang, et al., "Triboelectric Sensor Gloves for Real-Time Behavior Identification and Takeover Time Adjustment in Conditionally Automated Vehicles," *Nature Communications* 16, no. 1 (2025): 1080, <https://doi.org/10.1038/s41467-025-56169-2>.
221. Y. Liu, C. Yiu, Z. Song, et al., "Electronic Skin as Wireless Human-Machine Interfaces for Robotic VR," *Science Advances* 8, no. 2 (2022): eabl6700, <https://doi.org/10.1126/sciadv.abl6700>.
222. Q. Wang, Y. Li, Q. Xu, et al., "Finger-coding Intelligent Human-machine Interaction System Based on All-fabric Ionic Capacitive Pressure Sensors," *Nano Energy* 116 (2023): 108783, <https://doi.org/10.1016/j.nanoen.2023.108783>.
223. F. Wen, Z. Sun, T. He, et al., "Machine Learning Glove Using Self-Powered Conductive Superhydrophobic Triboelectric Textile for Gesture Recognition in VR/AR Applications," *Advanced Science* 7, no. 14 (2020): 2000261, <https://doi.org/10.1002/advs.202000261>.
224. Y. Zhou, S. Guo, Y. Zhou, et al., "Ionic Composite Nanofiber Membrane-Based Ultra-Sensitive and Anti-Interference Flexible Pressure Sensors for Intelligent Sign Language Recognition," *Advanced Functional Materials* 35, no. 29 (2025): 2425586, <https://doi.org/10.1002/adfm.202425586>.
225. H. Fang, J. Guo, and H. Wu, "Wearable Triboelectric Devices for Haptic Perception and VR/AR Applications," *Nano Energy* 96 (2022): 107112, <https://doi.org/10.1016/j.nanoen.2022.107112>.

226. J. Qi, F. Gao, G. Sun, J. C. Yeo, and C. T. Lim, "HaptGlove-Untethered Pneumatic Glove for Multimode Haptic Feedback in Reality-Virtuality Continuum," *Advanced Science* 10, no. 25 (2023): e2301044, <https://doi.org/10.1002/advs.202301044>.
227. M. Zhu, Z. Sun, Z. Zhang, et al., "Haptic-Feedback Smart Glove as a Creative Human-Machine Interface (HMI) for Virtual/Augmented Reality Applications," *Science Advances* 6, no. 19 (2020): eaaz8693, <https://doi.org/10.1126/sciadv.aaz8693>.
228. Y. Shi, F. Wang, J. Tian, et al., "Self-Powered Electro-Tactile System for Virtual Tactile Experiences," *Science Advances* 7, no. 6 (2021): eabe2943, <https://doi.org/10.1126/sciadv.abe2943>.
229. H. Dai, C. Zhang, C. Pan, et al., "Split-Type Magnetic Soft Tactile Sensor with 3D Force Decoupling," *Advanced Materials* 36, no. 11 (2024): e2310145, <https://doi.org/10.1002/adma.202310145>.
230. H. Zhao, Y. Zhang, L. Han, et al., "Intelligent Recognition Using Ultralight Multifunctional Nano-Layered Carbon Aerogel Sensors with Human-Like Tactile Perception," *Nano-Micro Letters* 16, no. 1 (2023): 11, <https://doi.org/10.1007/s40820-023-01216-0>.
231. H. Niu, X. Wei, H. Li, et al., "Micropyramid Array Bimodal Electronic Skin for Intelligent Material and Surface Shape Perception Based on Capacitive Sensing," *Advanced Science* 11, no. 3 (2024): e2305528, <https://doi.org/10.1002/advs.202305528>.
232. S. Yin, D. R. Yao, Y. Song, et al., "Wearable and Implantable Soft Robots," *Chemical Reviews* 124, no. 20 (2024): 11585–11636, <https://doi.org/10.1021/acs.chemrev.4c00513>.
233. Y. Li, L. Yang, S. Deng, et al., "A Machine Learning-Assisted Multifunctional Tactile Sensor for Smart Prosthetics," *InfoMat* 5, no. 9 (2023): e12463, <https://doi.org/10.1002/inf2.12463>.
234. L. Wen, M. Nie, J. Fan, et al., "Tactile Recognition of Shape and Texture on the Same Substrate," *Advanced Intelligent Systems* 5, no. 12 (2023): 2300337, <https://doi.org/10.1002/aisy.202300337>.
235. S. Wang, Y. Yao, W. Deng, et al., "Mass-Produced Skin-Inspired Piezoresistive Sensing Array with Interlocking Interface for Object Recognition," *ACS Nano* 18, no. 17 (2024): 11183–11192, <https://doi.org/10.1021/acsnano.4c00112>.
236. M. T. Francomano, D. Accoto, and E. Guglielmelli, "Artificial Sense of Slip—A Review," *IEEE Sensors Journal* 13, no. 7 (2013): 2489–2498, <https://doi.org/10.1109/jsen.2013.2252890>.
237. B. Nie, J. Geng, T. Yao, et al., "Sensing Arbitrary Contact Forces with a Flexible Porous Dielectric Elastomer," *Materials Horizons* 8, no. 3 (2021): 962–971, <https://doi.org/10.1039/d0mh01359e>.